

Mean Field Variational Bayes for Elaborate Distributions

Matthew P. Wand*, John T. Ormerod†, Simone A. Padoan‡ and Rudolf Frühwirth§

Abstract. We develop strategies for mean field variational Bayes approximate inference for Bayesian hierarchical models containing elaborate distributions. We loosely define elaborate distributions to be those having more complicated forms compared with common distributions such as those in the Normal and Gamma families. Examples are Asymmetric Laplace, Skew Normal and Generalized Extreme Value distributions. Such models suffer from the difficulty that the parameter updates do not admit closed form solutions. We circumvent this problem through a combination of (a) specially tailored auxiliary variables, (b) univariate quadrature schemes and (c) finite mixture approximations of troublesome density functions. An accuracy assessment is conducted and the new methodology is illustrated in an application.

Keywords: Auxiliary mixture sampling, Bayesian inference, Quadrature, Variational methods.

1 Introduction

We extend mean field variational Bayes (MFVB) so that Bayesian hierarchical models containing elaborate distributions can be accommodated. MFVB is a general approach to approximate inference in graphical models. Since Bayesian hierarchical models can be couched within the graphical models infrastructure, MFVB is a fast deterministic alternative to Markov chain Monte Carlo (MCMC) for approximate Bayesian inference. MFVB approximates the posterior density function of the parameter vector by restricting the space of candidate density functions to have a particular product structure, and

*School of Mathematical Sciences, University of Technology, Sydney, Broadway, Australia, <http://www.uow.edu.au/~mwand>

†School of Mathematics and Statistics, University of Sydney, Sydney, Australia, <http://www.maths.usyd.edu.au/u/jormerod/>

‡Department of Information Technology and Mathematical Methods, University of Bergamo, Dalmine, Italy, <http://www.unibg.it/pers/?simone.padoan>

§Institute of High Energy Physics, Austrian Academy of Sciences, Vienna, Austria, <http://www.hephy.at/user/fru/>

then maximizing a lower bound on the marginal likelihood over the restricted space via a coordinate ascent algorithm. We refer to the iterations of this algorithm as “updates”. The MFVB strategy results in fast and, for some models, quite accurate Bayesian inference. The idea originated in statistical physics (e.g., [Parisi 1988](#)), where it is known as *mean field theory*. It was developed as a methodology for inference in graphical models in the late 1990s (e.g., [Jordan et al. 1999](#), [Attias 1999](#)) and during the 2000s it permeated further into the mainstream statistical literature (e.g., [Teschendorff et al. 2005](#); [McGrory and Titterton 2007](#)). [Ormerod and Wand \(2010\)](#) contains a summary of MFVB from a statistical standpoint.

MFVB is one of many deterministic methods for approximate inference in graphical models which have become known as *variational methods*. An early survey of this topic is given by [Jordan et al. \(1999\)](#). Recently, [Wainwright and Jordan \(2008\)](#) showed that several deterministic algorithms, such as the sum-product algorithm (e.g., [Kschischang et al. 2001](#)), expectation propagation (e.g., [Minka 2001](#)) and semi-definite relaxations based on Lasserre sequences (e.g., [Lasserre 2001](#)), can be couched within the variational methodology framework. Varying degrees of accuracy can be achieved, depending on the level of sophistication of the variational method. For instance, the most tractable version of MFVB, in which the posterior distribution of the parameters are assumed to fully factorize, referred to as *naïve MFVB* in [Wainwright and Jordan \(2008\)](#), is susceptible to crude approximations. Improved performance results from treating various sub-vectors of the parameter vector as blocks in the MFVB product restriction. [Section 3](#) contains further details on the trade-off between tractability and accuracy.

A vital feature of MFVB, which allows it to be applied to a wide class of models, is the *locality property*. The locality property means that calculations concerning a particular parameter can be confined to ‘nearby’ parameters. It is best understood using graph theoretic representations of hierarchical Bayesian models, although we postpone the details on this to [Section 3](#). Gibbs sampling also possesses the locality property and the software package BUGS ([Lunn et al. 2000](#)) relies on it to efficiently handle highly complex models. Recently software packages that make use of the locality property of MFVB have emerged in an effort to streamline data analysis. The most prominent of these is Infer.NET ([Minka et al. 2010](#)) which is a suite of classes in .NET languages such as C#.

Despite these developments, the vast majority of MFVB methodology and software is restricted to models where the random components have common distributions such as

Normal, Gamma and Dirichlet, and the required calculations are analytic. This imposes quite stringent restrictions on the set of models that can be handled via MFVB. The current release of `Infer.NET` is subject to such restrictions.

In this article we explain how the class of distributions for variables in MFVB algorithms can be widened considerably. Specifically, we show how *elaborate* distributions such as t , Skew Normal, Asymmetric Laplace and Generalized Extreme Value can be handled within the MFVB framework. The incorporation of such distributions is achieved via a combination of

- specially tailored auxiliary variables,
- univariate quadrature schemes, and
- finite mixture approximation of troublesome density functions.

Auxiliary variables have already enjoyed some use in MFVB. Examples include [Tipping and Lawrence \(2003\)](#) for t -based robust curve fitting with fixed degrees of freedom, [Archanbeau and Bach \(2008\)](#) and [Armagan \(2009\)](#) for Laplace and other exponential power distributions and [Girolami and Rogers \(2006\)](#) and [Consonni and Marin \(2007\)](#) for binary response regression. Quadrature and finite mixture approximations have received little, if any, attention in the MFVB literature.

Quadrature is a classical numerical technique for evaluation of definite integrals that do not admit analytic solutions. A simple and effective form of quadrature is the trapezoidal rule which can be made arbitrarily accurate by increasing the number of trapezoidal elements. However, if the integral is over an infinite or semi-infinite region, rather than a compact interval, then it is important to determine the effective support of the integrand for accurate computation. Overflow and underflow is another concern with naïve application of the trapezoidal rule. Appendix B describes a quadrature-based numerical integration strategy that handles these potential problems.

We identify four distinct families of univariate integrals which arise in MFVB for the elaborate distributions treated here. The integrals within the families do not admit analytic solutions and quadrature is required. However, the integrands are well-behaved and we are able to tailor common quadrature schemes to achieve stable and accurate computation. Use of accurate quadrature schemes corresponds to more efficient MFVB updates than those based on Monte Carlo methods (e.g., Section 6.3 of [Winn and Bishop 2005](#)).

Auxiliary mixture sampling was introduced for a Bayesian analysis of stochastic volatility models by [Shephard \(1994\)](#) and has been applied in this context by, for example, [Kim et al. \(1998\)](#), [Chib et al. \(2002\)](#), and [Omori et al. \(2007\)](#). More recently, auxiliary mixture sampling has been extended to Bayesian inference for a broad class of models for discrete-valued data such as binary, categorical data, and count data, see, for example, [Frühwirth-Schnatter et al. \(2009\)](#) and [Frühwirth-Schnatter and Frühwirth \(2010\)](#). The approach involves approximation of particular density functions by finite, usually Normal, mixtures. The introduction of auxiliary indicator variables corresponding to components of the mixtures means that MCMC reduces to ordinary Gibbs sampling with closed form updates. The same idea is applicable to MFVB, and we use it for troublesome density functions such as those belonging to the Generalized Extreme Value family. A structured MFVB approach allows us to handle additional parameters such as the Generalized Extreme Value shape parameter.

Recently, [Braun and McAuliffe \(2010\)](#) used yet another approach, a version of the multivariate delta method, to handle elaborate distributions arising in discrete choice models.

We confine much of our discussion to univariate location-scale models, since the forms of many of the updates for multi-parameter extensions are essentially the same. The locality property of MFVB means that these forms are unchanged when embedded into larger models.

A critical issue of MFVB inference is accuracy compared with more exact approaches such as MCMC. We address this through a simulation study for a selection of elaborate distribution models. We find that the posterior densities of some parameters can be approximated very well. However the accuracy is only moderate to good for parameters which possess non-negligible posterior dependence with the introduced auxiliary variables. In particular, the spreads of posterior densities are often under-approximated (e.g., [Wang and Titterton 2005](#)).

Section 2 contains all definitions and distributional results used in this article. Section 3 summarizes MFVB and expands on the aforementioned locality property. In Section 4 we treat several location-scale models having elaborate distributional forms. Section 5 describes modifications when the alternative scale parameter priors are used. Extension to regression models is discussed in Section 6. In Section 7 we discuss extension to other elaborate distributions including discrete response models. The accuracy of MFVB for elaborate distribution models is assessed in Section 8. Section 9 applies some of the methodology developed in this paper to analysis of data from a respiratory

health study. Discussion of the methodology and its performance is given in Section 10. Three appendices provide technical details.

2 Definitions and Distributional Results

MFVB for elaborate distributions relies on several definitions and distributional results. We lay out each of them in this section. The results can be obtained via standard distribution theoretic manipulations.

2.1 Non-analytic Integral Families

A feature of MFVB for elaborate distributions is that not all calculations can be done analytically. Some univariate quadrature is required. The following integral families comprise the full set of non-analytic integrals which arise in the models considered in this article:

$$\mathcal{F}(p, q, r, s, t) \equiv \int_s^t x^p \exp \left[q \left\{ \frac{x}{2} \log \left(\frac{x}{2} \right) - \log \Gamma \left(\frac{x}{2} \right) \right\} - \frac{1}{2} r x \right] dx, \quad p \geq 0, \quad q, r, s, t > 0;$$

$$\mathcal{G}(p, q, r, s, t) \equiv \int_{-\infty}^{\infty} x^p (1 + x^2)^q \exp \left(-r x^2 + s x \sqrt{1 + x^2} + t x \right) dx \quad p, q \geq 0, \quad r > 0;$$

$$\mathcal{J}(p, q, r, s) \equiv \int_{-\infty}^{\infty} x^p \exp(qx - r x^2 - s e^{-x}) dx, \quad p \geq 0, \quad -\infty < q < \infty, \quad r, s > 0$$

and $\mathcal{J}^+(p, q, r) \equiv \int_0^{\infty} x^p \exp(qx - r x^2) dx, \quad p \geq 0, \quad -\infty < q < \infty, \quad r > 0.$

Since the integrals can take values that are arbitrarily large or small it is recommended that logarithmic storage and arithmetic be used, to avoid underflow and overflow. Appendix B discusses stable and efficient numerical computation of the members of each of these integral families.

Note that the last of these integrals can be expressed in terms of *parabolic cylinder functions*. Specifically,

$$\mathcal{J}^+(p, q, r) = (2r)^{-(p+1)/2} \Gamma(p+1) \exp\{q^2/(8r)\} D_{-p-1} \left(\frac{-q}{\sqrt{2r}} \right)$$

where D_ν is the parabolic cylinder function of order ν as defined in [Gradshteyn and Ryzhik \(1994\)](#). Software for computation of parabolic cylinder functions is available from web-sites associated with [Zhang and Jin \(1996\)](#). However, it is susceptible to underflow and overflow when $D_{-p-1}(-q/\sqrt{2r})$ is very small or large. The quadrature approach described in Appendix B overcomes this problem for general $\mathcal{J}^+(p, q, r)$.

2.2 Distributional Notation

The density function of a random vector \mathbf{v} in a Bayesian model is denoted by $p(\mathbf{v})$. The conditional density of \mathbf{v} given \mathbf{w} is denoted by $p(\mathbf{v}|\mathbf{w})$. The covariance matrix of \mathbf{v} is denoted by $\text{Cov}(\mathbf{v})$. If x_i has distribution D for each $1 \leq i \leq n$, and the x_i are independent, then we write $x_i \stackrel{\text{ind.}}{\sim} D$.

We use q to denote density functions that arise from MFVB approximation. For a generic random variable v and density function q we define:

$$\mu_{q(v)} \equiv E_q(v) \quad \text{and} \quad \sigma_{q(v)}^2 \equiv \text{Var}_q(v).$$

For a generic random vector \mathbf{v} and density function q we define:

$$\boldsymbol{\mu}_{q(\mathbf{v})} \equiv E_q(\mathbf{v}) \quad \text{and} \quad \boldsymbol{\Sigma}_{q(\mathbf{v})} \equiv \text{Cov}_q(\mathbf{v}).$$

2.3 Distributional Definitions

We use the common notation, $N(\mu, \sigma^2)$, for the Normal distribution with mean μ and variance σ^2 . The density and cumulative distribution functions of the $N(0, 1)$ distribution are denoted by ϕ and Φ , respectively. Furthermore, we write $(\phi/\Phi)(x) \equiv \phi(x)/\Phi(x)$ for the ratio of these two functions.

The Inverse-Gaussian density function with mean $\mu > 0$ and precision $\gamma > 0$ is given by

$$p(x; \mu, \gamma) = \gamma^{1/2} (2\pi x^3)^{-1/2} \exp \left\{ -\frac{\gamma(x - \mu)^2}{2\mu^2 x} \right\}, \quad x > 0.$$

We write Inverse-Gaussian(μ, γ) for the corresponding family of distributions.

Table 1 provides the functional forms for the densities that are used for modelling observed data in Section 4. For simplicity, we give the density with location μ equal to zero and scale σ equal to one. The general location and scale density function involves

the transition

$$f(x) \mapsto \frac{1}{\sigma} f\left(\frac{x - \mu}{\sigma}\right)$$

where $f(x)$ is as given in the second column of Table 1.

distribution	density in x ($\mu = 0, \sigma = 1$)	abbreviation
t	$\frac{\Gamma(\frac{\nu+1}{2})}{\sqrt{\pi\nu}\Gamma(\nu/2)(1+x^2/\nu)^{\frac{\nu+1}{2}}}$	$t(\mu, \sigma, \nu)$ ($\nu > 0$)
Asymmetric Laplace	$\tau(1-\tau)e^{-\frac{1}{2} x +(\tau-\frac{1}{2})x}$,	Asymmetric-Laplace(μ, σ, τ) ($0 < \tau < 1$)
Skew Normal	$2\phi(x)\Phi(\lambda x)$	Skew-Normal(μ, σ, λ)
Finite Normal Mixture	$(2\pi)^{-1/2} \sum_{k=1}^K (w_k/s_k) \times \phi((x - m_k)/s_k)$,	Normal-Mixture($\mu, \sigma, \mathbf{w}, \mathbf{m}, \mathbf{s}$) ($\sum_{k=1}^K w_k = 1, s_k > 0$)
Generalized Extreme Value	$(1 + \xi x)^{-1/\xi-1} \times e^{-(1+\xi x)^{-1/\xi}}$, $1 + \xi x > 0$	GEV(μ, σ, ξ)

Table 1: Density functions for modelling observed data. The functions ϕ and Φ are the density and cumulative distribution functions of the $N(0, 1)$ distribution. The scale parameter is subject to the restriction $\sigma > 0$ in all cases. The density function argument x and parameters range over \mathbb{R} unless otherwise specified.

For the t , Asymmetric Laplace, Skew Normal and Generalized Extreme Value distributions the shape parameters are, respectively, ν , τ , λ and ξ . The shape parameter for the Finite Normal Mixture family is the trio of K -vectors \mathbf{w} , \mathbf{m} and \mathbf{s} . The vector \mathbf{w} contains the Finite Normal Mixture weights, whilst \mathbf{m} and \mathbf{s} contain the means and standard deviations of each component. Figure 1 shows six members of each of the density families. The Finite Normal Mixture density functions are a selection of those defined in Table 1 of Marron and Wand (1992).

In Table 2 we describe density families that are used for modelling scale parameters in the upcoming examples. Note that the Half-Cauchy(A) distribution corresponds to

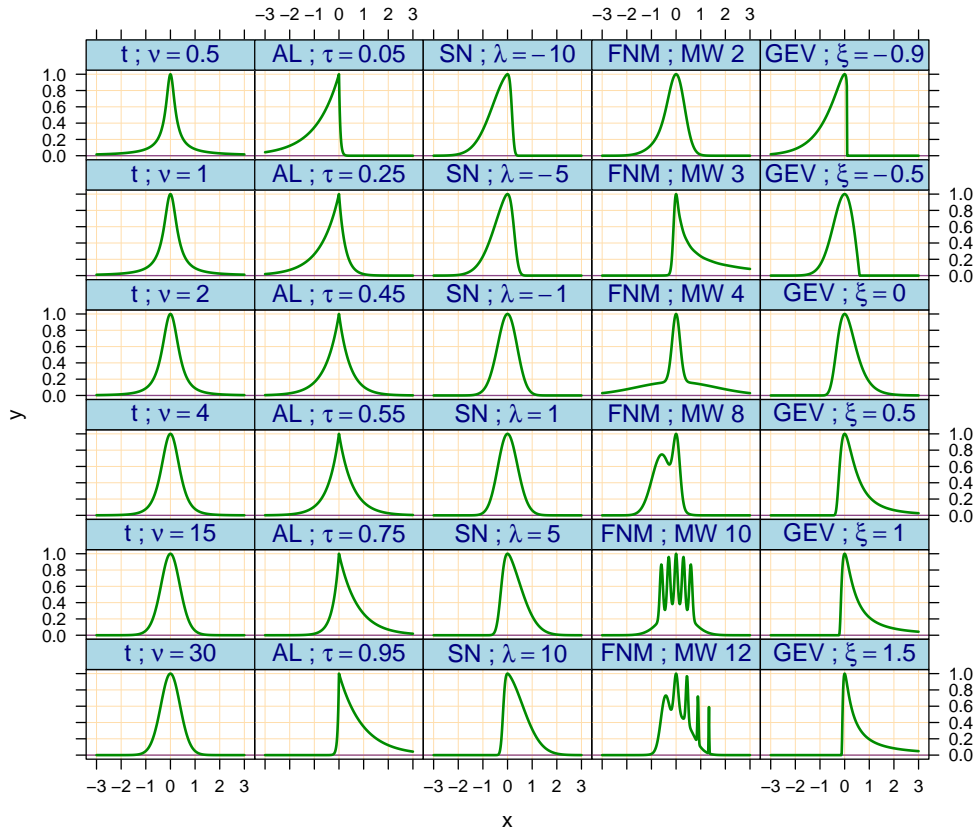


Figure 1: Example density functions for the families defined in Table 1 with varying values of the family's shape parameter. The location and scale parameters are chosen so that the mode of each density function has coordinates $(0, 1)$. The following abbreviations are used in the labels: AL for Asymmetric Laplace, SN for Skew Normal, FNM for Finite Normal Mixture and GEV for Generalized Extreme Value. For the Finite Normal Mixture density functions, the abbreviation 'MW n ' is shorthand for the shape parameter vectors \mathbf{w} , \mathbf{m} and \mathbf{s} corresponding to density number n in Table 1 of [Marron and Wand \(1992\)](#).

the Half- $t(A, 1)$ distribution.

distribution	density in x	abbreviation
Inverse Gamma	$\frac{B^A}{\Gamma(A)} x^{-A-1} e^{-B/x}$	Inverse-Gamma(A, B) ($A, B > 0$)
Log Normal	$\frac{1}{Bx\sqrt{2\pi}} \exp[-\frac{1}{2B^2} \{\log(x) - A\}^2]$	Log-Normal(A, B) ($B > 0$)
Half Cauchy	$\frac{2}{\pi A \{1 + (x/A)^2\}}$	Half-Cauchy(A) ($A > 0$)
Half t	$\frac{2\Gamma(\frac{\nu+1}{2})}{\sqrt{\pi\nu} \Gamma(\nu/2) A \{1 + (x/A)^2/\nu\}^{\frac{\nu+1}{2}}}$	Half- t (A, ν) ($A, \nu > 0$)

Table 2: Density functions used for modelling scale parameters. The density function argument x ranges over $x > 0$.

2.4 Distributional Results Involving Auxiliary Variables

In this section we give a collection of distributional results that link elaborate distributions to simpler ones. Each result is established in the literature, and straightforward to derive. However, they play vital roles in MFVB for elaborate distributions.

Result 1. *Let x and a be random variables such that*

$$x|a \sim N(\mu, a\sigma^2) \quad \text{and} \quad a \sim \text{Inverse-Gamma}(\frac{\nu}{2}, \frac{\nu}{2}).$$

Then $x \sim t(\mu, \sigma, \nu)$.

Result 1 is very well-known and used by, for example, [Lange et al. \(1989\)](#).

Result 2. *Let x and a be random variables such that*

$$x|a \sim N\left(\mu + \frac{(\frac{1}{2} - \tau)\sigma}{a\tau(1 - \tau)}, \frac{\sigma^2}{a\tau(1 - \tau)}\right) \quad \text{and} \quad a \sim \text{Inverse-Gamma}(1, \frac{1}{2}).$$

Then $x \sim \text{Asymmetric-Laplace}(\mu, \sigma, \tau)$.

Result 2 follows from Proposition 3.2.1 of [Kotz et al. \(2001\)](#).

Result 3. Let x and a be random variables such that

$$x|a \sim N\left(\mu + \frac{\sigma\lambda|a|}{\sqrt{1+\lambda^2}}, \frac{\sigma^2}{1+\lambda^2}\right) \quad \text{and} \quad a \sim N(0,1).$$

Then $x \sim \text{Skew-Normal}(\mu, \sigma, \lambda)$.

Result 3 is an immediate consequence of Proposition 3 of [Azzalini and Dalla Valle \(1996\)](#). These authors trace the result back to [Aigner et al. \(1977\)](#).

The next result involves the Multinomial($1; \boldsymbol{\pi}$) distribution where $\boldsymbol{\pi} = (\pi_1, \dots, \pi_K)$ is such that $\sum_{k=1}^K \pi_k = 1$. The corresponding probability mass function is

$$p(x_1, \dots, x_K) = \prod_{k=1}^K \pi_k^{x_k}, \quad x_k = 0, 1, \text{ for } 1 \leq k \leq K.$$

This result is very well-known and forms the basis of normal mixture fitting via the Expectation-Maximization algorithm (e.g., [Bishop 2006](#)).

Result 4. Let x be a random variable and \mathbf{a} be a $K \times 1$ random vector, having k th entry a_k , such that

$$p(x|\mathbf{a}) = \prod_{k=1}^K \left[(2\pi s_k^2)^{-1/2} \exp\left\{-\frac{1}{2}(x - m_k)^2/s_k^2\right\} \right]^{a_k}, \quad -\infty < x < \infty,$$

and $\mathbf{a} \sim \text{Multinomial}(1; \mathbf{w})$.

Then $x \sim \text{Normal-Mixture}(0, 1, \mathbf{w}, \mathbf{m}, \mathbf{s})$.

Our final result shows how a squared Half t random variable can be expressed as a scale mixture of Inverse Gamma random variables. This result is related to the classical representation of an F random variable as a scaled ratio of independent Chi-Squared random variables.

Result 5. Let x and a be random variables such that

$$x|a \sim \text{Inverse-Gamma}(\nu/2, \nu/a) \quad \text{and} \quad a \sim \text{Inverse-Gamma}\left(\frac{1}{2}, 1/A^2\right).$$

Then $\sqrt{x} \sim \text{Half-}t(A, \nu)$.

2.5 Expectation Results

The following expectation results are useful in some of the MFVB problems treated in Section 4. If $v \sim \text{Inverse-Gamma}(A, B)$ then

$$E(1/v) = A/B \quad \text{and} \quad E\{\log(v)\} = \log(B) - \text{digamma}(A).$$

If $v \sim \text{Inverse-Gaussian}(\mu, \gamma)$ then

$$E(v) = \mu \quad \text{and} \quad E(1/v) = \frac{1}{\mu} + \frac{1}{\gamma}. \tag{1}$$

3 Mean Field Variational Bayes

MFVB relies on product restrictions on posterior densities. This strategy also gives rise to the locality property that we discussed in Section 1. We now provide fuller details on MFVB and the locality property.

Consider the generic hierarchical Bayesian model:

$$\mathbf{x} | \theta_1, \theta_2, \theta_3 \sim p(\mathbf{x} | \theta_1, \theta_2, \theta_3),$$

$$\theta_1 | \theta_4 \sim p(\theta_1 | \theta_4), \quad \theta_2 | \theta_5, \theta_6 \sim p(\theta_2 | \theta_5, \theta_6), \quad \theta_3 | \theta_6 \sim p(\theta_3 | \theta_6) \quad \text{independently,} \tag{2}$$

$$\theta_4 \sim p(\theta_4), \quad \theta_5 \sim p(\theta_5), \quad \theta_6 \sim p(\theta_6) \quad \text{independently}$$

where \mathbf{x} is the observed data vector and

$$\boldsymbol{\theta} = (\theta_1, \theta_2, \theta_3, \theta_4, \theta_5, \theta_6)$$

is the vector of model parameters. For simplicity we assume that each of the θ_i assume values over a continuum so that (joint) posterior density functions, rather than posterior probability mass functions, are of central interest. The treatment of discrete-valued parameters is similar. MFVB strategies begin with postulation that the joint posterior density function $p(\mathbf{x} | \boldsymbol{\theta})$ is approximated by a particular product density form. Examples are

$$p(\boldsymbol{\theta} | \mathbf{x}) \approx q_{125}(\theta_1, \theta_2, \theta_5) q_{346}(\theta_3, \theta_4, \theta_6), \tag{3}$$

$$p(\boldsymbol{\theta} | \mathbf{x}) \approx q_{12}(\theta_1, \theta_2) q(\theta_5) q_{346}(\theta_3, \theta_4, \theta_6), \tag{4}$$

$$p(\boldsymbol{\theta} | \mathbf{x}) \approx q_{14}(\theta_1, \theta_4) q_{25}(\theta_2, \theta_5) q_{36}(\theta_3, \theta_6) \tag{5}$$

$$\text{and } p(\boldsymbol{\theta} | \mathbf{x}) \approx q_1(\theta_1) q_2(\theta_2) q_3(\theta_3) q_4(\theta_4) q_5(\theta_5) q_6(\theta_6). \tag{6}$$

Clearly there are very many options for the product density form, and the choice among them is typically made by trading off tractability against accuracy. Product density form (6), known as the *naïve* mean field approximation (Wainwright and Jordan 2008), will lead to the most tractable MFVB algorithm. But it is also the least accurate since it imposes the most stringent independence restriction on the approximation to $p(\boldsymbol{\theta}|\mathbf{x})$. Greater accuracy is achievable via less stringent product forms such as (3) and (4), but the updates may not be as tractable. It is also possible, due to the notion of *induced factorizations* (e.g., Bishop 2006, Section 10.2.5), that different product restrictions lead to identical MFVB approximations.

In keeping with the notational conventions declared in Section 2.2 we will, from now on, suppress the subscripts on the q density functions. The MFVB solutions can be shown to satisfy

$$q^*(\theta_i) \propto \exp\{E_{q(\boldsymbol{\theta}_{-i})}\log p(\theta_i|\mathbf{x}, \boldsymbol{\theta}_{-i})\}, \quad 1 \leq i \leq 6, \quad (7)$$

where $\boldsymbol{\theta}_{-i}$ denotes the set $\{\theta_1, \dots, \theta_6\}$ with θ_i excluded. Note that the expectation operator $E_{q(\boldsymbol{\theta}_{-i})}$ depends on the particular product density form being assumed. The optimal parameters in these q density functions can be determined by an iterative coordinate ascent scheme induced by (7) aimed at maximizing the lower bound on the marginal log-likelihood:

$$\log \underline{p}(\mathbf{x}; q) \equiv E_{q(\boldsymbol{\theta})}\{\log p(\mathbf{x}, \boldsymbol{\theta}) - \log q(\boldsymbol{\theta})\} \leq \log p(\mathbf{x}).$$

If it is assumed that each iteration entails unique maximization of $\log \underline{p}(\mathbf{x}; q)$ with respect to the current θ_i , and that the search is restricted to a compact set, then convergence to a local maximizer of $\log \underline{p}(\mathbf{x}; q)$ is guaranteed (Luenberger and Ye 2008, p. 253). Successive values of $\log \underline{p}(\mathbf{x}; q)$ can be used to monitor convergence. At convergence $q^*(\theta_i)$, $1 \leq i \leq 6$, and $\log \underline{p}(\mathbf{x}; q)$ are, respectively, the minimum Kullback-Leibler approximations to the posterior densities $p(\theta_i|\mathbf{x})$, $1 \leq i \leq 6$, and the marginal log-likelihood $\log p(\mathbf{x})$.

The extension to general Bayesian models with arbitrary parameter vectors and latent variables is straightforward. Summaries may be found in, for example, Chapter 10 of Bishop (2006) and Ormerod and Wand (2010). As described in these references, directed acyclic graph (DAG) representations of Bayesian hierarchical models are very useful when deriving MFVB schemes for large models. We make use of DAG representations in the remainder of this section. Each panel of Figure 2 displays the DAG of model (2).

It remains to explain the locality property of MFVB. From graphical model theory

(Pearl 1988) we have the result

$$p(\theta_i|\mathbf{x}, \boldsymbol{\theta}_{-i}) = p(\theta_i|\text{Markov blanket of } \theta_i)$$

where the Markov blanket of a node on a DAG is the set of parents, co-parents and children of that node. From this result we get the following simplification of (7):

$$q^*(\theta_i) \propto \exp\{E_{q(\boldsymbol{\theta}_{-i})}\log p(\theta_i|\text{Markov blanket of } \theta_i)\}, \quad 1 \leq i \leq 6. \quad (8)$$

The locality property of MFVB is encapsulated in Result (8). It affords considerable simplification for the model at hand, but also allows MFVB results for one model to be transferred to another. We now explain this graphically.

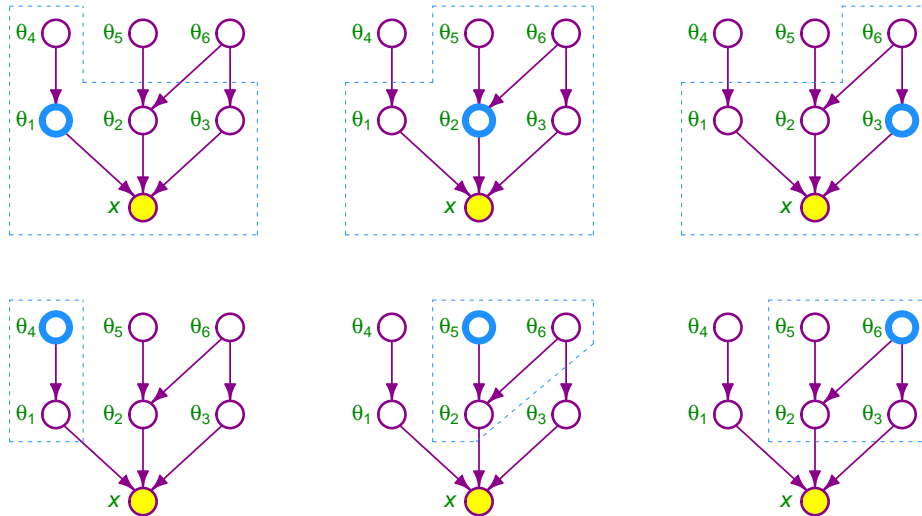


Figure 2: Markov blankets for each of the six parameters (hidden nodes) in the example Bayesian hierarchical model (directed acyclic graph), given by (2). In each panel the Markov blanket is shown for the thick-circled blue node, using dashed lines. The shaded node \mathbf{x} corresponds to the observed data (evidence node).

The panels in Figure 2 show the Markov blankets for the each of $\theta_1, \dots, \theta_6$. The θ_i are known as *hidden nodes* in graphical models parlance and the data vector \mathbf{x} comprises the *evidence node*. The arrows convey conditional dependence among the random variables in the model. The Markov blanket for θ_1 is $\{\theta_2, \theta_3, \theta_4, \mathbf{x}\}$, which means that $q^*(\theta_1)$ depends on particular q -density moments of θ_2, θ_3 and θ_4 , but not on their distributions.

If, for example, $p(\theta_2|\theta_5)$ is changed from Inverse-Gamma(0.07, θ_5) to Log-Normal(25, θ_5) then this will not impact upon the form of $q^*(\theta_1)$. The MFVB solution for $q^*(\theta_4)$ provides a more dramatic illustration of the locality property, since the Markov blanket of θ_4 is simply $\{\theta_1\}$. This means that $q^*(\theta_4)$ is unaffected by the likelihood $p(\mathbf{x}|\theta_1, \theta_2, \theta_3)$. Therefore, results established for $q^*(\theta_4)$ for, say, $x_i|\theta_1, \theta_2, \theta_3 \stackrel{\text{ind.}}{\sim} t(\theta_1, \theta_2, \theta_3)$ also apply to $x_i|\theta_1, \theta_2, \theta_3 \stackrel{\text{ind.}}{\sim} \text{GEV}(\theta_1, \theta_2, \theta_3)$.

The upshot of the locality property of MFVB is that we can restrict attention to the simplest versions of models involving elaborate distributions with the knowledge that the forms that arise also apply to larger models. For this reason, Section 4 deals only with such models.

3.1 Extension to Structured Mean Field Variational Bayes

We now describe an extension of MFVB known as *structured* MFVB. It involves breaking down graphical models for which direct MFVB is difficult into sub-components for which MFVB is tractable. Structured MFVB was first proposed by [Saul and Jordan \(1996\)](#) and, subsequently, has been used in various Machine Learning contexts such as coupled hidden Markov models ([Jaakkola 2001](#)). To the best of our knowledge, the present article is the first to use structured MFVB for approximate statistical inference in hierarchical Bayesian models. Therefore, we will explain the concept in the context of such models. We will do this by building on the description of MFVB hierarchical Bayesian models that we gave in Section 2.2 of [Ormerod and Wand \(2010\)](#).

Consider the Bayesian model

$$\mathbf{x}|\boldsymbol{\theta}, \eta \sim p(\mathbf{x}|\boldsymbol{\theta}, \eta) \tag{9}$$

where $\boldsymbol{\theta} \in \Theta$ and $\eta \in N$. The partition of the parameter space is such that MFVB inference for $\boldsymbol{\theta}$ is tractable when η is fixed at a constant, but is not tractable when the full model (9) applies and η is a model parameter. For the purposes of this explanation we will suppose that $\boldsymbol{\theta}$ is a continuous parameter vector, but that η is discrete. Other cases have similar treatment. Let $p(\boldsymbol{\theta})$, $\boldsymbol{\theta} \in \Theta$, denote the prior density function of $\boldsymbol{\theta}$ and $p(\eta)$, $\eta \in N$ denote the prior probability mass function of η .

Let $q(\boldsymbol{\theta}, \eta)$ be a general density/probability mass function in $(\boldsymbol{\theta}, \eta)$. The Kullback-Leibler-based lower bound on the marginal log-likelihood is

$$\log \underline{p}(\mathbf{x}; q) = \sum_{\eta \in N} \int_{\Theta} q(\boldsymbol{\theta}, \eta) \log \left\{ \frac{p(\mathbf{x}, \boldsymbol{\theta}, \eta)}{q(\boldsymbol{\theta}, \eta)} \right\} d\boldsymbol{\theta}$$

(cf. (4) of Ormerod and Wand, 2010). For each $\eta \in N$ suppose that we approximate the posterior density function of $\boldsymbol{\theta}$ as follows:

$$p(\boldsymbol{\theta}, \eta | \mathbf{x}) \approx q(\eta) \prod_{i=1}^M q(\boldsymbol{\theta}_i | \eta)$$

where $\{\boldsymbol{\theta}_1, \dots, \boldsymbol{\theta}_M\}$ is a partition of $\boldsymbol{\theta}$. Then the lower bound on the marginal log-likelihood becomes

$$\log \underline{p}(\mathbf{x}; q) = \sum_{\eta \in N} q(\eta) \left[\int_{\Theta} q(\boldsymbol{\theta} | \eta) \log \left\{ \frac{p(\mathbf{x}, \boldsymbol{\theta} | \eta)}{q(\boldsymbol{\theta} | \eta)} \right\} d\boldsymbol{\theta} + \log \left\{ \frac{p(\eta)}{q(\eta)} \right\} \right].$$

Using arguments similar to those in the ordinary MFVB situation (see e.g., Section 2.2 of Ormerod and Wand 2010, where similar notation is used) the optimal $q(\boldsymbol{\theta}_i | \eta)$ densities satisfy

$$q^*(\boldsymbol{\theta}_i | \eta) \propto \exp\{E_{q(\boldsymbol{\theta}_{-i} | \eta)} \log p(\boldsymbol{\theta}_i | \mathbf{x}, \boldsymbol{\theta}_{-i}, \eta)\}, \quad 1 \leq i \leq M, \quad \eta \in N.$$

As before, $\boldsymbol{\theta}_{-i}$ denotes $\boldsymbol{\theta}$ with the $\boldsymbol{\theta}_i$ component omitted. It follows that $q^*(\boldsymbol{\theta}_i | \eta)$ densities can be found by applying the MFVB coordinate ascent algorithm separately for each $\eta \in N$. Upon substitution of these solutions into the marginal log-likelihood lower bound we obtain

$$\log \underline{p}(\mathbf{x}; q^*(\cdot | \eta)) = \sum_{\eta \in N} q(\eta) \log \left\{ \underline{p}(\mathbf{x}, \eta) / q(\eta) \right\} \tag{10}$$

where

$$\underline{p}(\mathbf{x}, \eta) \equiv \underline{p}(\mathbf{x} | \eta) p(\eta) \equiv \int_{\boldsymbol{\theta}} q^*(\boldsymbol{\theta} | \eta) \log \left\{ \frac{p(\mathbf{x}, \boldsymbol{\theta} | \eta)}{q^*(\boldsymbol{\theta} | \eta)} \right\} d\boldsymbol{\theta} p(\eta).$$

The minimizer of (10) over $q(\eta)$ is (e.g., Result 1 of Ormerod and Wand 2010)

$$q^*(\eta) = \underline{p}(\eta | \mathbf{x}) = \frac{p(\eta) \underline{p}(\mathbf{x} | \eta)}{\sum_{\eta' \in N} p(\eta') \underline{p}(\mathbf{x} | \eta')}.$$

The overall approximations of $p(\boldsymbol{\theta}_i | \mathbf{x})$ and $\log p(\mathbf{x})$ are then

$$q^*(\boldsymbol{\theta}_i) \equiv \sum_{\eta \in N} q^*(\eta) q^*(\boldsymbol{\theta}_i | \eta) \quad \text{and} \quad \underline{p}(\mathbf{x}; q) \equiv \sum_{\eta \in N} q^*(\eta) \underline{p}(\mathbf{x} | \eta).$$

4 Univariate Location-Scale Models

Consider univariate Bayesian models of the form

$$x_1, \dots, x_n | \mu, \sigma, \boldsymbol{\theta} \stackrel{\text{ind.}}{\sim} \frac{1}{\sigma} f\left(\frac{x - \mu}{\sigma}; \boldsymbol{\theta}\right) \tag{11}$$

where f is a fixed density function, $\mu \in \mathbb{R}$ is the location parameter, $\sigma > 0$ is the scale parameter and $\boldsymbol{\theta} \in \Theta$ is a set of shape parameters. We call (11) a *univariate location-scale model*.

We will take the prior on μ to be Gaussian:

$$\mu \sim N(\mu_\mu, \sigma_\mu^2), \quad -\infty < \mu_\mu < \infty, \quad \sigma_\mu^2 > 0$$

throughout this article. Gaussian priors for location parameters are generally adequate, and have a straightforward multi-parameter extension. Prior specification for scale parameters is somewhat more delicate (Gelman 2006). In the current section we take the prior for σ to be of the form

$$p(\sigma) \propto \sigma^{-2A-1} e^{-B/\sigma^2}, \quad A, B > 0. \quad (12)$$

This is equivalent to the squared scale, σ^2 , having an Inverse-Gamma prior. Due to conjugacy relationships between the Gaussian and Inverse-Gamma families, use of (12) results in MFVB algorithms with fewer intractable integrals. In Section 5 we treat alternative scale parameter priors. Let $p(\boldsymbol{\theta})$ denote the prior on $\boldsymbol{\theta}$. The form of $p(\boldsymbol{\theta})$ will change from one model to another.

The exact posterior density function for μ is

$$p(\mu|\mathbf{x}) = \frac{\exp\{-\frac{1}{2\sigma_\mu^2}(\mu - \mu_\mu)^2\} \int_{\Theta} \int_0^\infty \sigma^{-n} \prod_{i=1}^n f\{(x_i - \mu)/\sigma; \boldsymbol{\theta}\} d\sigma d\boldsymbol{\theta}}{\int_{-\infty}^\infty \exp\{-\frac{1}{2\sigma_\mu^2}(\mu - \mu_\mu)^2\} \int_{\Theta} \int_0^\infty \sigma^{-n} \prod_{i=1}^n f\{(x_i - \mu)/\sigma; \boldsymbol{\theta}\} d\sigma d\boldsymbol{\theta} d\mu}.$$

Similar expressions arise for $p(\sigma|\mathbf{x})$ and $p(\boldsymbol{\theta}|\mathbf{x})$. For elaborate f forms, the integrals in the normalizing factors are almost always intractable. For multi-parameter extensions we get stuck with multivariate integrals of arbitrary dimension.

The remainder of this section involves case-by-case treatment of the univariate location-scale models that arise when f is set to each of the densities in Table 1. These cases allow illustration of the difficulties that arise in MFVB inference for elaborate distributions, and our strategy for overcoming them. Discussion concerning other f forms is given in Section 7.

For each univariate location model we

- specify the product restriction that defines the form of the MFVB approximation,
- describe a coordinate ascent algorithm for determining the solution, and
- provide the lower bound on the marginal log-likelihood for monitoring convergence.

4.1 *t* Model

A Bayesian *t* model for a univariate random sample is

$$\begin{aligned}
 x_i | \mu, \sigma, \nu &\stackrel{\text{ind.}}{\sim} t(\mu, \sigma, \nu), \\
 \mu &\sim N(\mu_\mu, \sigma_\mu^2), \quad \sigma^2 \sim \text{Inverse-Gamma}(A, B), \quad \nu \sim \text{Uniform}(\nu_{\min}, \nu_{\max})
 \end{aligned}
 \tag{13}$$

where μ_μ and $A, B, \nu_{\min}, \nu_{\max}, \sigma_\mu^2 > 0$ are hyperparameters. For low values of $\nu > 0$, the *t* distribution has very heavy tails, so it is commonly used to model data containing gross outliers. This aspect of model (13) and its regression extensions (Section 6) translates to attractive robustness properties (e.g., Lange et al. 1989). Section 9 contains a nonparametric regression example that uses the *t* distribution to achieve robustness.

Using Result 1 we can re-write (13) as

$$\begin{aligned}
 x_i | a_i, \mu, \sigma &\stackrel{\text{ind.}}{\sim} N(\mu, a_i \sigma^2), \quad a_i | \nu \stackrel{\text{ind.}}{\sim} \text{Inverse-Gamma}\left(\frac{\nu}{2}, \frac{\nu}{2}\right), \\
 \mu &\sim N(\mu_\mu, \sigma_\mu^2), \quad \sigma^2 \sim \text{Inverse-Gamma}(A, B), \quad \nu \sim \text{Uniform}(\nu_{\min}, \nu_{\max}).
 \end{aligned}$$

For MFVB inference we impose the product restriction

$$q(\mu, \sigma, \nu, \mathbf{a}) = q(\mu, \nu)q(\sigma)q(\mathbf{a}).$$

This yields the following forms for the optimal densities:

$$\begin{aligned}
 q^*(\mu) &\sim N(\mu_{q(\mu)}, \sigma_{q(\mu)}^2) \\
 q^*(\sigma^2) &\sim \text{Inverse-Gamma}\left(A + \frac{n}{2}, B + \frac{1}{2} \sum_{i=1}^n \mu_{q(1/a_i)} \{(x_i - \mu_{q(\mu)})^2 + \sigma_{q(\mu)}^2\}\right) \\
 q^*(a_i) &\stackrel{\text{ind.}}{\sim} \text{Inverse-Gamma}\left(\frac{\mu_{q(\nu)} + 1}{2}, \frac{1}{2} \left[\mu_{q(\nu)} + \mu_{q(1/\sigma^2)} \{(x_i - \mu_{q(\mu)})^2 + \sigma_{q(\mu)}^2\} \right]\right) \\
 q^*(\nu) &= \frac{\exp\left[n \left\{ \frac{\nu}{2} \log(\nu/2) - \log \Gamma(\nu/2) \right\} - (\nu/2) C_1\right]}{\mathcal{F}(0, n, C_1, \nu_{\min}, \nu_{\max})}, \quad \nu_{\min} < \nu < \nu_{\max}.
 \end{aligned}
 \tag{14}$$

The last density uses the definition: $C_1 \equiv \sum_{i=1}^n \{\mu_{q(\log a_i)} + \mu_{q(1/a_i)}\}$. The parameters in (14) are determined from Algorithm 2. Appendix A.1 contains the derivations of (14) and the parameter update expressions.

Algorithm 2: Coordinate ascent scheme for obtaining the parameters in the optimal densities $q^*(\mathbf{a})$, $q^*(\mu)$, $q^*(\nu)$ and $q^*(\sigma)$ for the t model.

Initialize: $\mu_{q(\mu)} \in \mathbb{R}$, $\sigma_{q(\mu)}^2 > 0$, $\mu_{q(\nu)} \in [\nu_{\min}, \nu_{\max}]$ and $\mu_{q(1/\sigma^2)} > 0$.

Cycle:

For $i = 1, \dots, n$:

$$B_{q(a_i)} \leftarrow \frac{1}{2} \left[\mu_{q(\nu)} + \mu_{q(1/\sigma^2)} \{ (x_i - \mu_{q(\mu)})^2 + \sigma_{q(\mu)}^2 \} \right]$$

$$\mu_{q(1/a_i)} \leftarrow \frac{1}{2} (\mu_{q(\nu)} + 1) / B_{q(a_i)}$$

$$\mu_{q(\log a_i)} \leftarrow \log(B_{q(a_i)}) - \text{digamma}\left(\frac{1}{2}(\mu_{q(\nu)} + 1)\right)$$

$$\sigma_{q(\mu)}^2 \leftarrow \left(\mu_{q(1/\sigma^2)} \sum_{i=1}^n \mu_{q(1/a_i)} + \frac{1}{\sigma_{\mu}^2} \right)^{-1}$$

$$\mu_{q(\mu)} \leftarrow \sigma_{q(\mu)}^2 \left(\mu_{q(1/\sigma^2)} \sum_{i=1}^n x_i \mu_{q(1/a_i)} + \frac{\mu_{\mu}}{\sigma_{\mu}^2} \right)$$

$$C_1 \leftarrow \sum_{i=1}^n \{ \mu_{q(\log a_i)} + \mu_{q(1/a_i)} \}$$

$$\mu_{q(\nu)} \leftarrow \exp\{ \log \mathcal{F}(1, n, C_1, \nu_{\min}, \nu_{\max}) - \log \mathcal{F}(0, n, C_1, \nu_{\min}, \nu_{\max}) \}$$

$$B_{q(\sigma^2)} \leftarrow B + \frac{1}{2} \sum_{i=1}^n \mu_{q(1/a_i)} \{ (x_i - \mu_{q(\mu)})^2 + \sigma_{q(\mu)}^2 \} \quad ; \quad \mu_{q(1/\sigma^2)} \leftarrow \frac{A + \frac{n}{2}}{B_{q(\sigma^2)}}$$

until the increase in $\underline{p}(\mathbf{x}; q)$ is negligible.

An explicit expression for $\log \underline{p}(\mathbf{x}; q)$ is:

$$\begin{aligned} \log \underline{p}(\mathbf{x}; q) = & \frac{1}{2} - \frac{n}{2} \log(2\pi) + \frac{1}{2} \log(\sigma_{q(\mu)}^2 / \sigma_\mu^2) - \frac{(\mu_{q(\mu)} - \mu_\mu)^2 + \sigma_{q(\mu)}^2}{2\sigma_\mu^2} \\ & + A \log(B) - \log \Gamma(A) - (A + \frac{n}{2}) \log(B_{q(\sigma^2)}) + \log \Gamma(A + \frac{n}{2}) \\ & + \log \mathcal{F}(0, n, C_1, \nu_{\min}, \nu_{\max}) - \log(\nu_{\max} - \nu_{\min}) + n \log \Gamma(\frac{1}{2}(\mu_{q(\nu)} + 1)) \\ & + \frac{1}{2} \mu_{q(\nu)} \sum_{i=1}^n \mu_{q(\log a_i)} + \sum_{i=1}^n B_{q(a_i)} \mu_{q(1/a_i)} - \frac{1}{2} (\mu_{q(\nu)} + 1) \sum_{i=1}^n \log \{B_{q(a_i)}\} \end{aligned}$$

although it is only valid after each of the updates in Algorithm 2 have been performed.

Figure 3 shows the results from application of Algorithm 2 to a simulated data set of size $n = 500$ from the $t(4, 0.5, 1.5)$ distribution. The algorithm was terminated when the relative increase in $\log \underline{p}(\mathbf{x}; q)$ was less than 10^{-6} . As shown in the first panel of Figure 3, this required about 75 iterations. The true parameter values are within the high probability regions of each approximate posterior density function, and this tended to occur for other realizations of the simulated data.

4.2 Asymmetric Laplace Model

The Asymmetric Laplace model for a univariate random sample is

$$x_i | \mu, \sigma \stackrel{\text{ind.}}{\sim} \text{Asymmetric-Laplace}(\mu, \sigma, \tau), \tag{15}$$

$$\mu \sim N(\mu_\mu, \sigma_\mu^2), \quad \sigma^2 \sim \text{Inverse-Gamma}(A, B)$$

where $\mu_\mu \in \mathbb{R}$ and $A, B, \sigma_\mu^2 > 0$ are hyperparameters.

We treat the case where the asymmetry parameter $0 < \tau < 1$ is a fixed number to be specified by the user. Note that, μ equals the τ quantile of the distribution of the x_i s. Regression model extensions of (15), of the type described in Section 6, correspond to Bayesian quantile regression (Yu and Moyeed 2001). Laplacian variables also arise in Bayesian representations of the lasso (Park and Casella 2008) and wavelet-based nonparametric regression (Antoniadis and Fan 2001).

Using Result 2 we can re-write model (15) as

$$x_i | a_i, \mu, \sigma \stackrel{\text{ind.}}{\sim} N\left(\mu + \frac{(\frac{1}{2} - \tau)\sigma}{a_i \tau (1 - \tau)}, \frac{\sigma^2}{a_i \tau (1 - \tau)}\right), \quad a_i \stackrel{\text{ind.}}{\sim} \text{Inverse-Gamma}(1, \frac{1}{2}),$$

$$\mu \sim N(\mu_\mu, \sigma_\mu^2), \quad \sigma^2 \sim \text{Inverse-Gamma}(A, B).$$

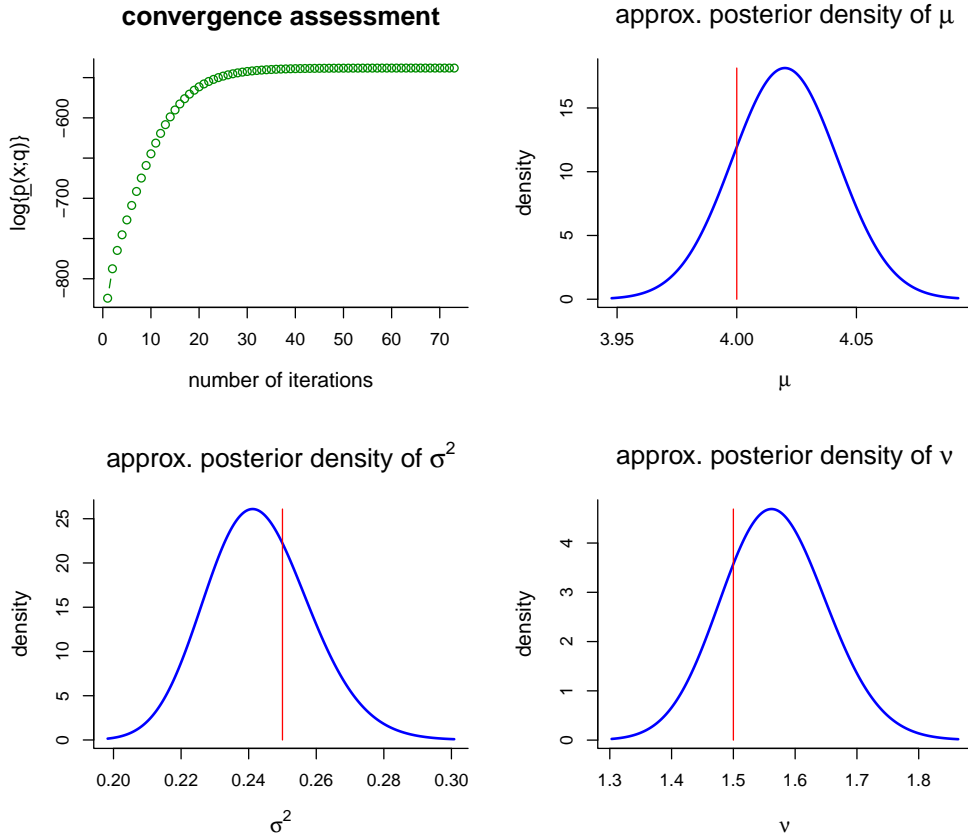


Figure 3: Results of application of Algorithm 2 to a simulated random sample of size $n = 500$ from the $t(4, 0.5, 1.5)$ distribution. The upper-left panel shows successive values of $\log p(\mathbf{x}; q)$, up until the meeting of a stringent convergence criterion. The other panels show the approximate posterior density functions for the three model parameters. The vertical lines correspond to the true values of the parameters from which the data were generated.

For MFVB inference we impose the product restriction

$$q(\mu, \sigma, \mathbf{a}) = q(\mu)q(\sigma)q(\mathbf{a}). \quad (16)$$

The optimal densities take the forms:

$$\begin{aligned}
 q^*(\mu) &\sim N(\mu_{q(\mu)}, \sigma_{q(\mu)}^2), \\
 q^*(\sigma) &= \frac{\sigma^{-(2A+n+1)} \exp(C_2/\sigma - C_3/\sigma^2)}{\mathcal{J}^+(2A+n-1, C_2, C_3)}, \quad \sigma > 0 \\
 \text{and } q^*(a_i) &\stackrel{\text{ind.}}{\sim} \text{Inverse-Gaussian}(\mu_{q(a_i)}, \{4\tau(1-\tau)\}^{-1}).
 \end{aligned}$$

The parameters are determined from Algorithm 3. See Appendix A.2 for the derivations.

An expression for $\log \underline{p}(\mathbf{x}; q)$, valid at the bottom of the loop in Algorithm 3, is:

$$\begin{aligned}
 \log \underline{p}(\mathbf{x}; q) &= \frac{1}{2} + \log(2) + n \log\{\tau(1-\tau)\} - \frac{\sum_{i=1}^n \{1/\mu_{q(a_i)}\}}{8\tau(1-\tau)} + \frac{1}{2} \log(\sigma_{q(\mu)}^2 / \sigma_\mu^2) \\
 &\quad - \frac{(\mu_{q(\mu)} - \mu_\mu)^2 + \sigma_{q(\mu)}^2}{2\sigma_\mu^2} + A \log(B) - \log \Gamma(A) \\
 &\quad + \log \mathcal{J}^+(2A+n-1, C_2, C_3).
 \end{aligned}$$

4.3 Skew Normal Model

A Bayesian Skew Normal model for a univariate random sample is

$$x_i | \mu, \sigma \stackrel{\text{ind.}}{\sim} \text{Skew-Normal}(\mu, \sigma, \lambda), \tag{17}$$

$$\mu \sim N(\mu_\mu, \sigma_\mu^2), \quad \sigma^2 \sim \text{Inverse-Gamma}(A, B), \quad \lambda \sim N(\mu_\lambda, \sigma_\lambda^2)$$

where $\mu_\mu, \mu_\lambda \in \mathbb{R}$ and $A, B, \sigma_\mu^2, \sigma_\lambda^2 > 0$ are hyperparameters. Model (17) is based on the version of the Skew Normal distribution used by [Azzalini and Dalla Valle \(1996\)](#). The Skew Normal distribution can be used to model skewed data when it is desirable to have the Normal distribution as a special case. This distribution also arises from the bivariate normal distribution when one component is conditioned on the other being positive and, hence, is appropriate for modelling data arising from such a mechanism.

Using Result 3 we can re-write model (17) as

$$\begin{aligned}
 x_i | a_i, \mu, \sigma, \lambda &\stackrel{\text{ind.}}{\sim} N\left(\mu + \frac{\lambda |a_i|}{\sqrt{1+\lambda^2}}, \frac{\sigma^2}{1+\lambda^2}\right), \quad a_i \stackrel{\text{ind.}}{\sim} N(0, 1), \\
 \mu &\sim N(\mu_\mu, \sigma_\mu^2), \quad \sigma^2 \sim \text{Inverse-Gamma}(A, B), \quad \lambda \sim N(\mu_\lambda, \sigma_\lambda^2).
 \end{aligned}$$

Algorithm 3: Coordinate ascent scheme for obtaining the parameters in the optimal densities $q^*(\mathbf{a})$, $q^*(\mu)$ and $q^*(\sigma)$ for the Asymmetric Laplace model.

Initialize: $\mu_{q(\mu)} \in \mathbb{R}$ and $\sigma_{q(\mu)}^2, \mu_{q(1/\sigma)}, \mu_{q(1/\sigma^2)} > 0$.

Cycle:

For $i = 1, \dots, n$:

$$\mu_{q(a_i)} \leftarrow \left[4\tau^2(1-\tau)^2 \mu_{q(1/\sigma^2)} \{ (x_i - \mu_{q(\mu)})^2 + \sigma_{q(\mu)}^2 \} \right]^{-1/2}.$$

$$\mu_{q(1/a_i)} \leftarrow 1/\mu_{q(a_i)} + 4\tau(1-\tau)$$

$$\sigma_{q(\mu)}^2 \leftarrow \{ \tau(1-\tau) \mu_{q(1/\sigma^2)} \sum_{i=1}^n \mu_{q(a_i)} + 1/\sigma_{\mu}^2 \}^{-1}$$

$$\mu_{q(\mu)} \leftarrow \sigma_{q(\mu)}^2 \left\{ \tau(1-\tau) \mu_{q(1/\sigma^2)} \sum_{i=1}^n x_i \mu_{q(a_i)} + n(\tau - \frac{1}{2}) \mu_{q(1/\sigma)} + \mu_{\mu} / \sigma_{\mu}^2 \right\}$$

$$C_2 \leftarrow n(\bar{x} - \mu_{q(\mu)}) (\frac{1}{2} - \tau)$$

$$C_3 \leftarrow B + \frac{1}{2} \tau (1 - \tau) \sum_{i=1}^n \mu_{q(a_i)} \{ (x_i - \mu_{q(\mu)})^2 + \sigma_{q(\mu)}^2 \}$$

$$\mu_{q(1/\sigma^2)} \leftarrow \exp\{ \log \mathcal{J}^+(2A + n + 1, C_2, C_3) - \log \mathcal{J}^+(2A + n - 1, C_2, C_3) \}$$

$$\mu_{q(1/\sigma)} \leftarrow \exp\{ \log \mathcal{J}^+(2A + n, C_2, C_3) - \log \mathcal{J}^+(2A + n - 1, C_2, C_3) \}$$

until the increase in $\underline{p}(\mathbf{x}; q)$ is negligible.

For MFVB inference we impose the product restriction

$$q(\mu, \sigma, \lambda, \mathbf{a}) = q(\mu)q(\sigma)q(\lambda)q(\mathbf{a}).$$

This leads to the following forms for the optimal densities:

$$\begin{aligned} q^*(\mu) &\sim N(\mu_{q(\mu)}, \sigma_{q(\mu)}^2) \\ q^*(\sigma) &= \frac{\sigma^{-(2A+n+1)} \exp(C_4/\sigma - C_5/\sigma^2)}{\mathcal{J}^+(2A+n-1, C_4, C_5)} \\ q^*(\lambda) &= \frac{(1+\lambda^2)^{n/2} \exp\{-C_6\lambda^2 + C_7\lambda\sqrt{1+\lambda^2} + (\mu_\lambda/\sigma_\lambda^2)\lambda\}}{\mathcal{G}(0, \frac{1}{2}n, C_6, C_7, (\mu_\lambda/\sigma_\lambda^2))}, \quad -\infty < \lambda < \infty \\ \text{and } q^*(\mathbf{a}) &= \prod_{i=1}^n \frac{\sqrt{1+\mu_{q(\lambda^2)}} \exp\{-\frac{1}{2}(1+\mu_{q(\lambda^2)})a_i^2 + C_{i8}|a_i|\}}{2(\Phi/\phi)(C_{i8}/\sqrt{1+\mu_{q(\lambda^2)}})}, \quad -\infty < a_i < \infty. \end{aligned}$$

The parameters are determined from Algorithm 4. Justification is provided in Appendix A.3.

Note the simplified expression for use in Algorithm 4:

$$\begin{aligned} \log \underline{p}(\mathbf{x}; q) &= \frac{1}{2} + n \log(2) - (n + \frac{1}{2}) \log(2\pi) + A \log(B) - \log \Gamma(A) \\ &\quad - \frac{(\mu_{q(\mu)} - \mu_\mu)^2 + \sigma_{q(\mu)}^2}{2\sigma_\mu^2} + \frac{1}{2} \log(\sigma_{q(\mu)}^2/\sigma_\mu^2) - \frac{1}{2} \log(\sigma_\lambda^2) - \frac{\mu_\lambda^2}{2\sigma_\lambda^2} \\ &\quad + \frac{1}{2} \mu_{q(\lambda^2)} \left[\mu_{q(1/\sigma^2)} \left\{ \sum_{i=1}^n (x_i - \mu_{q(\mu)})^2 + \sigma_{q(\mu)}^2 \right\} + \sum_{i=1}^n \mu_{q(a_i^2)} \right] \\ &\quad + \log \mathcal{G}(0, \frac{1}{2}n, \frac{1}{2}C_6, C_7, (\mu_\lambda/\sigma_\lambda^2)) + \log \mathcal{J}^+(2A+n-1, C_4, C_5) \\ &\quad + n \log(2) + \sum_{i=1}^n \log \mathcal{J}^+(0, C_{i8}, \frac{1}{2}(1+\mu_{q(\lambda^2)})). \end{aligned}$$

4.4 Finite Normal Mixture Model

Consider the model

$$x_i | \mu, \sigma \stackrel{\text{ind.}}{\sim} \text{Normal-Mixture}(\mu, \sigma; \mathbf{w}, \mathbf{m}, \mathbf{s}), \tag{18}$$

$$\mu \sim N(\mu_\mu, \sigma_\mu^2), \quad \sigma^2 \sim \text{Inverse-Gamma}(A, B)$$

where μ_μ and $A, B, \sigma_\mu^2 > 0$ are hyperparameters. In model (18), \mathbf{w}, \mathbf{m} and \mathbf{s} are each *fixed* vectors and do not require Bayesian inference. Hence, we are *not* concerned

Algorithm 4: Coordinate ascent scheme for obtaining the parameters in the optimal densities q_a^* , $q^*(\mu)$, $q^*(\sigma)$ and $q^*(\lambda)$ for the Skew Normal model.

Initialize: $\mu_{q(\mu)} \in \mathbb{R}$ and $\sigma_{q(\mu)}^2, \mu_{q(1/\sigma)}, \mu_{q(1/\sigma^2)} > 0$.

Cycle:

For $i = 1, \dots, n$:

$$C_{i8} \leftarrow \mu_{q(1/\sigma)} \mu_{q(\lambda\sqrt{1+\lambda^2})} (x_i - \mu_{q(\mu)})$$

$$\mu_{q(|a_i|)} \leftarrow \frac{C_{i8}}{1+\mu_{q(\lambda^2)}} + \frac{(\phi/\Phi)(C_{i8}/\sqrt{1+\mu_{q(\lambda^2)}})}{\sqrt{1+\mu_{q(\lambda^2)}}}$$

$$\mu_{q(a_i^2)} \leftarrow \frac{1+\mu_{q(\lambda^2)}+C_{i8}^2}{(1+\mu_{q(\lambda^2)})^2} + \frac{C_{i8}(\phi/\Phi)(C_{i8}/\sqrt{1+\mu_{q(\lambda^2)}})}{(1+\mu_{q(\lambda^2)})\sqrt{1+\mu_{q(\lambda^2)}}}$$

$$\sigma_{q(\mu)}^2 \leftarrow \left\{ \frac{1}{\sigma_\mu^2} + n\mu_{q(1/\sigma^2)}(1 + \mu_{q(\lambda^2)}) \right\}^{-1}$$

$$\mu_{q(\mu)} \leftarrow \sigma_{q(\mu)}^2 \left\{ \frac{\mu_\mu}{\sigma_\mu^2} + n\mu_{q(1/\sigma^2)}(1 + \mu_{q(\lambda^2)}) \bar{x} - \mu_{q(1/\sigma)} \mu_{q(\lambda\sqrt{1+\lambda^2})} \sum_{i=1}^n \mu_{q(|a_i|)} \right\}$$

$$C_4 \leftarrow \mu_{q(\lambda\sqrt{1+\lambda^2})} \sum_{i=1}^n \mu_{q(|a_i|)} (x_i - \mu_{q(\mu)})$$

$$C_5 \leftarrow B + \frac{1}{2}(1 + \mu_{q(\lambda^2)}) \left\{ \sum_{i=1}^n (x_i - \mu_{q(\mu)})^2 + n\sigma_{q(\mu)}^2 \right\}$$

$$\mu_{q(1/\sigma^2)} \leftarrow \frac{\mathcal{J}^+(2A+n+1, C_4, C_5)}{\mathcal{J}^+(2A+n-1, C_4, C_5)} \quad ; \quad \mu_{q(1/\sigma)} \leftarrow \frac{\mathcal{J}^+(2A+n, C_4, C_5)}{\mathcal{J}^+(2A+n-1, C_4, C_5)}$$

$$C_6 \leftarrow \mu_{q(1/\sigma^2)} \left\{ \sum_{i=1}^n (x_i - \mu_{q(\mu)})^2 + n\sigma_{q(\mu)}^2 \right\} + \sum_{i=1}^n \mu_{q(a_i^2)} + \frac{1}{\sigma_\lambda^2}$$

$$C_7 \leftarrow \mu_{q(1/\sigma)} \sum_{i=1}^n \mu_{q(|a_i|)} (x_i - \mu_{q(\mu)}).$$

$$\mu_{q(\lambda^2)} \leftarrow \exp\{\log\mathcal{G}(2, \frac{1}{2}n, \frac{1}{2}C_6, C_7, (\mu_\lambda/\sigma_\lambda^2)) - \log\mathcal{G}(0, \frac{1}{2}n, \frac{1}{2}C_6, C_7, (\mu_\lambda/\sigma_\lambda^2))\}$$

$$\mu_{q(\lambda\sqrt{1+\lambda^2})} \leftarrow \exp\{\log\mathcal{G}(1, \frac{1}{2}(n+1), \frac{1}{2}C_6, C_7, (\mu_\lambda/\sigma_\lambda^2)) - \log\mathcal{G}(0, \frac{1}{2}n, \frac{1}{2}C_6, C_7, (\mu_\lambda/\sigma_\lambda^2))\}$$

until the increase in $p(\mathbf{x}; q)$ is negligible.

with the classical normal mixture fitting problem in this section. Model (18) is not of great interest in its own right. However, as illustrated in Section 4.5, it becomes relevant when a troublesome response variable density function is replaced by an accurate normal mixture approximation.

Using Result 4 we can rewrite model (18) as

$$p(\mathbf{x} | \mu, \sigma, \mathbf{a}_i) = \prod_{i=1}^n \prod_{k=1}^K \left[\sigma^{-1} (2\pi s_k^2)^{-1/2} \exp \left\{ -\frac{1}{2} \left(\frac{x_i - \mu}{\sigma} - m_k \right)^2 / s_k^2 \right\} \right]^{a_{ik}},$$

$$\mathbf{a}_i \stackrel{\text{ind.}}{\sim} \text{Multinomial}(1; \mathbf{w}), \quad \mu \sim N(\mu_\mu, \sigma_\mu^2), \quad \sigma^2 \sim \text{Inverse-Gamma}(A, B)$$

and a_{ik} denotes the k th entry of \mathbf{a}_i . The auxiliary random vectors \mathbf{a}_i , $1 \leq i \leq n$, facilitate more tractable MFVB calculations as is apparent from the derivations given in Appendix A.4. Under the product restriction

$$q(\mu, \sigma, \mathbf{a}) = q(\mu)q(\sigma)q(\mathbf{a})$$

the optimal densities take the form:

$$\begin{aligned} q^*(\mu) &\sim N(\mu_{q(\mu)}, \sigma_{q(\mu)}^2), \\ q^*(\sigma) &= \frac{\sigma^{-2A-n-1} \exp(C_9/\sigma - C_{10}/\sigma^2)}{\mathcal{J}^+(2A+n-1, C_9, C_{10})}, \quad \sigma > 0, \\ \text{and } q^*(\mathbf{a}_i) &\stackrel{\text{ind.}}{\sim} \text{Multinomial}(1; \boldsymbol{\mu}_{q(\mathbf{a}_i)}). \end{aligned}$$

The parameters are determined from Algorithm 5. Appendix A.4 contains the derivations.

An explicit expression for $\log p(\mathbf{x}; q)$ is:

$$\begin{aligned} \log p(\mathbf{x}; q) &= \frac{1}{2} - \frac{n}{2} \log(2\pi) + \log(2) + A \log(B) - \log \Gamma(A) \\ &\quad + \log \mathcal{J}^+(2A+n-1, C_9, C_{10}, 0) \\ &\quad + \sum_{k=1}^K \mu_{q(a_{\bullet k})} \left\{ \log(w_k) - \frac{1}{2} \log(s_k^2) - \frac{1}{2} (m_k^2/s_k^2) \right\} \\ &\quad + \frac{1}{2} \log \left(\frac{\sigma_{q(\mu)}^2}{\sigma_\mu^2} \right) - \frac{(\mu_{q(\mu)} - \mu_\mu)^2 + \sigma_{q(\mu)}^2}{2\sigma_\mu^2} - \sum_{i=1}^n \sum_{k=1}^K \mu_{q(a_{ik})} \log(\mu_{q(a_{ik})}). \end{aligned}$$

Algorithm 5: Coordinate ascent scheme for obtaining the parameters in the optimal densities $q^*(\mathbf{a})$, $q^*(\mu)$ and $q^*(\sigma)$ for the Finite Normal Mixture model.

Initialize: $\mu_{q(\mu)} \in \mathbb{R}$ and $\sigma_{q(\mu)}^2, \mu_{q(1/\sigma)}, \mu_{q(1/\sigma^2)} > 0$

Cycle:

For $i = 1, \dots, n, k = 1, \dots, K$:

$$\nu_{ik} \leftarrow \log(w_k) - \frac{1}{2} \log(s_k^2) - \frac{1}{2s_k^2} \left[\mu_{q(1/\sigma^2)} \{ (x_i - \mu_{q(\mu)})^2 + \sigma_{q(\mu)}^2 \} - 2\mu_{q(1/\sigma)} m_k (x_i - \mu_{q(\mu)}) + m_k^2 \right]$$

For $i = 1, \dots, n, k = 1, \dots, K$: $\mu_{q(a_{ik})} \leftarrow \exp(\nu_{ik}) / \sum_{k=1}^K \exp(\nu_{ik})$

For $k = 1, \dots, K$: $\mu_{q(a_{\bullet k})} \leftarrow \sum_{i=1}^n \mu_{q(a_{ik})}$

$$\sigma_{q(\mu)}^2 \leftarrow \left(1/\sigma_\mu^2 + \mu_{q(1/\sigma^2)} \sum_{k=1}^K \frac{\mu_{q(a_{\bullet k})}}{s_k^2} \right)^{-1}$$

$$\mu_{q(\mu)} \leftarrow \sigma_{q(\mu)}^2 \left\{ \mu_{q(1/\sigma^2)} \sum_{i=1}^n \sum_{k=1}^K \frac{\mu_{q(a_{ik})} x_i}{s_k^2} - \mu_{q(1/\sigma)} \sum_{k=1}^K \frac{\mu_{q(a_{\bullet k})} m_k}{s_k^2} + \frac{\mu_\mu}{\sigma_\mu^2} \right\}$$

$$C_9 \leftarrow \sum_{i=1}^n \sum_{k=1}^K \frac{\mu_{q(a_{ik})} m_k (x_i - \mu_{q(\mu)})}{s_k^2}$$

$$C_{10} \leftarrow B + \frac{1}{2} \sum_{i=1}^n \sum_{k=1}^K \frac{\mu_{q(a_{ik})} \{ (x_i - \mu_{q(\mu)})^2 + \sigma_{q(\mu)}^2 \}}{s_k^2}$$

$$\mu_{q(1/\sigma^2)} \leftarrow \exp\{ \log \mathcal{J}^+(2A + n + 1, C_9, C_{10}) - \log \mathcal{J}^+(2A + n - 1, C_9, C_{10}) \}$$

$$\mu_{q(1/\sigma)} \leftarrow \exp\{ \log \mathcal{J}^+(2A + n, C_9, C_{10}) - \log \mathcal{J}^+(2A + n - 1, C_9, C_{10}) \}$$

until the increase in $p(\mathbf{x}; q)$ is negligible.

4.5 Generalized Extreme Value Model

Now consider the case where f is the standard Generalized Extreme Value density function with shape parameter $-\infty < \xi < \infty, \xi \neq 0$:

$$f(x; \xi) = (1 + \xi x)^{-1/\xi - 1} e^{-(1 + \xi x)^{-1/\xi}}, \quad 1 + \xi x > 0.$$

Letting $\xi \rightarrow 0$ results in the standard Gumbel density

$$f(x; 0) = \exp(-x - e^{-x}), \quad -\infty < x < \infty.$$

The Generalized Extreme Value distribution is commonly used to model sample extremes.

Direct MFVB is problematic for the location-scale model (11) when f is $GEV(0, 1, \xi)$, since the likelihood induced by $f(\cdot; \xi)$ has complicated dependence on the parameters. A reasonable way out is to work with normal mixture approximations to the $f(\cdot; \xi)$:

$$f(x; \xi) \approx \sum_{k=1}^K \frac{w_{k,\xi}}{s_{k,\xi}} \phi\left(\frac{x - m_{k,\xi}}{s_{k,\xi}}\right). \tag{19}$$

Approximations for $f(x; 0)$ have been employed successfully by [Frühwirth-Schnatter and Wagner \(2006\)](#) for Markov chain Monte Carlo-based inference. A number of extensions of this work now exist, such as [Frühwirth-Schnatter et al. \(2009\)](#). In Appendix C we describe normal mixture approximation for other members of the $GEV(0, 1, \xi)$ family of density functions.

Let Ξ be a finite parameter space for the ξ parameter and consider the univariate GEV location-scale model:

$$x_i | \mu, \sigma \stackrel{\text{ind.}}{\sim} GEV(\mu, \sigma, \xi), \tag{20}$$

$$\mu \sim N(\mu_\mu, \sigma_\mu^2), \quad \sigma^2 \sim \text{Inverse-Gamma}(A, B), \quad \xi \sim p(\xi)$$

where $\mu_\mu \in \mathbb{R}$ and $A, B, \sigma_\mu^2 > 0$ are hyperparameters and $p(\xi)$ is a fixed probability mass function over $\xi \in \Xi$.

For any fixed $\xi \in \Xi$, suppose we have a normal mixture approximation to $f(\cdot; \xi)$. Then we can use Algorithm 5 to obtain MFVB approximations, with the restrictions

$$q(\mu, \sigma, \xi) = q(\xi)q(\mu|\xi)q(\sigma|\xi).$$

Let these approximations be denoted by $q^*(\mu|\xi)$ and $q^*(\sigma|\xi)$, respectively.

Using results from Section 3.1 with $\theta = (\mu, \sigma)$ and $\eta = \xi$ we get the structured MFVB approximations

$$q^*(\xi) \equiv \frac{p(\xi)\underline{p}(\mathbf{x}|\xi)}{\sum_{\xi' \in \Xi} p(\xi')\underline{p}(\mathbf{x}|\xi')}, \quad q^*(\mu) \equiv \sum_{\xi \in \Xi} q^*(\xi)q^*(\mu|\xi) \quad \text{and} \quad q^*(\sigma) \equiv \sum_{\xi \in \Xi} q^*(\xi)q^*(\sigma|\xi).$$

The approximate marginal log-likelihood is

$$\underline{p}(\mathbf{x}; q) \equiv \sum_{\xi \in \Xi} q^*(\xi)\underline{p}(\mathbf{x}|\xi).$$

Algorithm 6 summarizes this structured MFVB approach to inference for (μ, σ, ξ) in (20). The algorithm assumes that finite normal mixture approximations of the form (19) have been obtained for each $\xi \in \Xi$. Such calculations only need to be done once and can be stored in a look-up table. As described in Appendix C, we have done them for $\xi \in \{-1, -0.995, \dots, 0.995, 1\}$ with $K = 24$.

Algorithm 6: Structured MFVB scheme for approximation of the posteriors $p(\xi|\mathbf{x})$, $p(\mu|\mathbf{x})$ and $p(\sigma|\mathbf{x})$ for the Generalized Extreme Value model.

For each $\xi \in \Xi$:

1. Retrieve the normal mixture approximation vectors: $(w_{k,\xi}, m_{k,\xi}, s_{k,\xi})$, $1 \leq k \leq K$, for approximation of the $\text{GEV}(0, 1, \xi)$ density function.
2. Apply Algorithm 5 with (w_k, m_k, s_k) set to $(w_{k,\xi}, m_{k,\xi}, s_{k,\xi})$, $1 \leq k \leq K$.
3. Store the parameters needed to define $q^*(\mu|\xi)$ and $q^*(\sigma|\xi)$.
4. Store the converged marginal likelihood lower bound $\underline{p}(\mathbf{x}|\xi)$.

Form the approximations to the posteriors $p(\xi|\mathbf{x})$, $p(\mu|\mathbf{x})$ and $p(\sigma|\mathbf{x})$ as follows:

$$q^*(\xi) = \frac{p(\xi)\underline{p}(\mathbf{x}|\xi)}{\sum_{\xi' \in \Xi} p(\xi')\underline{p}(\mathbf{x}|\xi')}, \quad q^*(\mu) = \sum_{\xi \in \Xi} q^*(\xi)q^*(\mu|\xi), \quad q^*(\sigma) = \sum_{\xi \in \Xi} q^*(\xi)q^*(\sigma|\xi).$$

4.6 General Univariate Location-Scale Models

As demonstrated in the previous section for the GEV univariate location-scale model, the auxiliary normal mixture approach offers itself as a viable ‘last resort’ for trouble-

some density functions. Provided f in (11) is reasonably smooth, one can approximate it arbitrarily well by a finite normal mixture and then use Algorithm 5. If additional parameters are present, such as the GEV shape parameter ξ , then there is the option of imposing a discrete finite prior and using the approach exemplified by Algorithm 6.

Hence, the auxiliary mixture approach can be used for MFVB inference for general univariate location-scale models.

5 Alternative Scale Parameter Priors

The Inverse Gamma distribution is the conjugate family for variance parameters in Normal mean-scale models. Since, after the introduction of auxiliary variables, many of the models in Section 4 involve Normal distributions the conjugacy property helps reduce the number of non-analytic forms. However, alternative scale parameter priors are often desirable. Gelman (2006) argues that Half t densities are better for achieving non-informativeness of scale parameters, and pays particular attention to Half Cauchy scale priors. The Bayesian variable selection models of Cottet et al. (2008) use Log Normal priors for scale parameters. In this section we briefly describe the handling of these alternative scale parameter priors in MFVB inference.

5.1 Half t Prior

Consider the following alternative to (13):

$$x_i | \mu, \sigma \stackrel{\text{ind.}}{\sim} t(\mu, \sigma, \nu), \tag{21}$$

$$\mu \sim N(\mu_\mu, \sigma_\mu^2), \quad \sigma \sim \text{Half-}t(A, \omega), \quad \nu \sim \text{Uniform}(\nu_{\min}, \nu_{\max})$$

where $\mu_\mu \in \mathbb{R}$ and $\sigma_\mu^2, A, \omega, \nu_{\min}, \nu_{\max} > 0$ are hyperparameters. The only difference is $\sigma^2 \sim \text{Inverse-Gamma}(A, B)$ is replaced with $\sigma \sim \text{Half-}t(A, \omega)$. As before, we introduce auxiliary variables of the form $a_i | \nu \stackrel{\text{ind.}}{\sim} \text{Inverse-Gamma}(\frac{\nu}{2}, \frac{\nu}{2})$. In addition, we introduce $b \sim \text{Inverse-Gamma}(\frac{1}{2}, 1/A^2)$. Then Results 1 and 5 allow us to write (21) as

$$x_i | a_i, \mu, \sigma \stackrel{\text{ind.}}{\sim} N(\mu, a_i \sigma^2), \quad a_i | \nu \stackrel{\text{ind.}}{\sim} \text{Inverse-Gamma}(\frac{\nu}{2}, \frac{\nu}{2}),$$

$$\mu \sim N(\mu_\mu, \sigma_\mu^2), \quad \sigma^2 | b \sim \text{Inverse-Gamma}(\omega/2, \omega/b),$$

$$b \sim \text{Inverse-Gamma}(\frac{1}{2}, 1/A^2), \quad \nu \sim \text{Uniform}(\nu_{\min}, \nu_{\max}).$$

The optimal q densities are the same as (14), but with

$$q^*(\sigma^2) \sim \text{Inverse-Gamma} \left(\frac{n + \omega}{2}, \omega \mu_{q(1/b)} + \frac{1}{2} \sum_{i=1}^n \mu_{q(1/a_i)} \{ (x_i - \mu_{q(\mu)})^2 + \sigma_{q(\mu)}^2 \} \right).$$

The optimal parameters can be obtained using a coordinate ascent algorithm similar to Algorithm 2. The only change is that

$$B_{q(\sigma^2)} \leftarrow B + \frac{1}{2} \sum_{i=1}^n \mu_{q(1/a_i)} \{ (x_i - \mu_{q(\mu)})^2 + \sigma_{q(\mu)}^2 \} ; \quad \mu_{q(1/\sigma^2)} \leftarrow \frac{A + \frac{n}{2}}{B_{q(\sigma^2)}}$$

is replaced with

$$\mu_{q(1/b)} \leftarrow \frac{1}{2} (\omega + 1) A^2 \{ \omega A^2 \mu_{q(1/\sigma^2)} + 1 \}^{-1} ;$$

$$B_{q(\sigma^2)} \leftarrow \omega \mu_{q(1/b)} + \frac{1}{2} \sum_{i=1}^n \mu_{q(1/a_i)} \{ (x_i - \mu_{q(\mu)})^2 + \sigma_{q(\mu)}^2 \} ; \quad \mu_{q(1/\sigma^2)} \leftarrow \frac{n + \omega}{2 B_{q(\sigma^2)}}.$$

The expression for $\log p(\underline{\mathbf{x}}; q)$ becomes:

$$\begin{aligned} \log p(\underline{\mathbf{x}}; q) &= \frac{1}{2} - \frac{n}{2} \log(2\pi) + \frac{1}{2} \log(\sigma_{q(\mu)}^2 / \sigma_\mu^2) - \frac{(\mu_{q(\mu)} - \mu_\mu)^2 + \sigma_{q(\mu)}^2}{2\sigma_\mu^2} + \frac{1}{2} \omega \log(\omega) \\ &\quad + \log \Gamma(\frac{1}{2}(n + \omega)) + \log \Gamma(\frac{1}{2}(\omega + 1)) - \log \Gamma(\omega/2) - \frac{1}{2} \log(\pi) - \log(A) \\ &\quad - \frac{1}{2}(n + \omega) \log \{ B_{q(\sigma^2)} \} - \frac{1}{2}(\omega + 1) \log \{ \omega \mu_{q(1/\sigma^2)} + A^{-2} \} \\ &\quad + \omega \mu_{q(1/b)} \mu_{q(1/\sigma^2)} + \log \mathcal{F}(0, n, C_1, \nu_{\min}, \nu_{\max}) - \log(\nu_{\max} - \nu_{\min}) \\ &\quad + n \log \Gamma(\frac{1}{2}(\mu_{q(\nu)} + 1)) + \frac{1}{2} \mu_{q(\nu)} \sum_{i=1}^n \mu_{q(\log a_i)} + \sum_{i=1}^n B_{q(a_i)} \mu_{q(1/a_i)} \\ &\quad - \frac{1}{2}(\mu_{q(\nu)} + 1) \sum_{i=1}^n \log \{ B_{q(a_i)} \}. \end{aligned}$$

5.2 Log Normal Prior

Next, consider the following alternative to (13):

$$x_i | \mu, \sigma \stackrel{\text{ind.}}{\sim} t(\mu, \sigma, \nu),$$

$$\mu \sim N(\mu_\mu, \sigma_\mu^2), \quad \sigma \sim \text{Log-Normal}(A, B), \quad \nu \sim \text{Uniform}(\nu_{\min}, \nu_{\max})$$

where $\mu_\mu \in \mathbb{R}$ and $A, B, \nu_{\min}, \nu_{\max}, \sigma_\mu^2 > 0$ are hyperparameters. Once again, we introduce auxiliary variables $a_i | \nu \stackrel{\text{ind.}}{\sim} \text{Inverse-Gamma}(\frac{\nu}{2}, \frac{\nu}{2})$, and work with

$$x_i | a_i, \mu, \sigma \stackrel{\text{ind.}}{\sim} N(\mu, a_i \sigma^2).$$

The optimal q densities are the same as (14), but with

$$q^*(\sigma) = \frac{2\sigma^{(A/B^2)-n-1} \exp\{-C_{11}/\sigma^2 - (\log\sigma)^2/(2B^2)\}}{\mathcal{J}(0, \frac{A}{2B^2} - \frac{n}{2}, \frac{1}{8B^2}, C_{11})}, \quad \sigma > 0.$$

The optimal parameters can be obtained using a coordinate ascent algorithm similar to Algorithm 2. The only change is that

$$B_{q(\sigma^2)} \leftarrow B + \frac{1}{2} \sum_{i=1}^n \mu_{q(1/a_i)} \{(x_i - \mu_{q(\mu)})^2 + \sigma_{q(\mu)}^2\} \quad ; \quad \mu_{q(1/\sigma^2)} \leftarrow \frac{A + \frac{n}{2}}{B_{q(\sigma^2)}}$$

is replaced with

$$C_{11} \leftarrow \frac{1}{2} \sum_{i=1}^n \mu_{q(1/a_i)} \{(x_i - \mu_{q(\mu)})^2 + \sigma_{q(\mu)}^2\} \quad ; \quad \mu_{q(1/\sigma^2)} \leftarrow \frac{\mathcal{J}(0, \frac{A}{2B^2} - 1 - \frac{n}{2}, \frac{1}{8B^2}, C_{11})}{\mathcal{J}(0, \frac{A}{2B^2} - \frac{n}{2}, \frac{1}{8B^2}, C_{11})}.$$

The expression for $\log p(\mathbf{x}; q)$ becomes:

$$\begin{aligned} \log p(\mathbf{x}; q) &= \frac{n+1}{2} + \frac{n}{2} \mu_{q(\nu)} - \frac{n}{2} \log(2\pi) + \frac{1}{2} \log(\sigma_{q(\mu)}^2 / \sigma_\mu^2) - \frac{(\mu_{q(\mu)} - \mu_\mu)^2 + \sigma_{q(\mu)}^2}{2\sigma_\mu^2} \\ &\quad - \frac{1}{2} \log(2\pi) - \frac{1}{2} (A^2/B^2) - \log(B) + \log \mathcal{J}(0, \frac{A}{2B^2} - \frac{n}{2}, \frac{1}{8B^2}, C_{11}) \\ &\quad + \log \mathcal{F}(0, n, C_1, \nu_{\min}, \nu_{\max}) - \log(\nu_{\max} - \nu_{\min}) \\ &\quad + n \log \Gamma(\frac{1}{2}(\mu_{q(\nu)} + 1)) - \frac{n}{2} (\mu_{q(\nu)} + 1) \operatorname{digamma}\{\frac{1}{2}(\mu_{q(\nu)} + 1)\}. \end{aligned}$$

6 Extension to Regression Models

Up until now we have restricted attention to univariate models. This has the advantage that the various issues that arise with elaborate distributions in MFVB can be addressed with minimal notational effort. The locality property of MFVB means that the non-analytic forms that were identified in Sections 4 and 5 still apply for larger models. In this section we examine the most common multiparameter extension: from univariate models to regression models. For shape parameters such as ν , the t distribution degrees of freedom, this extension has no impact on the updates. The scale parameter updates are only mildly impacted. The location parameter μ is replaced by a vector of regression coefficients β . Algebraically, this involves replacement of

$$\mathbf{1}\mu \quad \text{by} \quad \mathbf{X}\beta$$

in the model specification. The updates for β then involve matrix algebraic counterparts of $\mu_{q(\mu)}$ and $\sigma_{q(\mu)}^2$. We will provide details on this extension for the t -distribution model with Inverse Gamma priors. Extensions for other models are similar.

A Bayesian t regression model (e.g., Lange et al. 1989) is

$$y_i | \boldsymbol{\beta}, \sigma \stackrel{\text{ind.}}{\sim} t((\mathbf{X}\boldsymbol{\beta})_i, \sigma, \nu), \quad (22)$$

$$\boldsymbol{\beta} \sim N(\boldsymbol{\mu}_\beta, \boldsymbol{\Sigma}_\beta), \quad \sigma^2 \sim \text{Inverse-Gamma}(A, B), \quad \nu \sim \text{Uniform}(\nu_{\min}, \nu_{\max})$$

where $\boldsymbol{\mu}_\beta$ and $\boldsymbol{\Sigma}_\beta$ hyperparameters for $\boldsymbol{\beta}$. We can re-write (22) as

$$y_i | a_i, \mu, \sigma \stackrel{\text{ind.}}{\sim} N((\mathbf{X}\boldsymbol{\beta})_i, a_i \sigma^2), \quad a_i | \nu \stackrel{\text{ind.}}{\sim} \text{Inverse-Gamma}(\frac{\nu}{2}, \frac{\nu}{2}),$$

$$\boldsymbol{\beta} \sim N(\boldsymbol{\mu}_\beta, \boldsymbol{\Sigma}_\beta), \quad \sigma^2 \sim \text{Inverse-Gamma}(A, B), \quad \nu \sim \text{Uniform}(\nu_{\min}, \nu_{\max}).$$

For MFVB inference we impose the product restriction

$$q(\boldsymbol{\beta}, \sigma, \nu, \mathbf{a}) = q(\boldsymbol{\beta}, \nu)q(\sigma)q(\mathbf{a}).$$

This yields the following forms for the optimal densities:

$$\begin{aligned} q^*(\boldsymbol{\beta}) &\sim N(\boldsymbol{\mu}_{q(\boldsymbol{\beta})}, \boldsymbol{\Sigma}_{q(\boldsymbol{\mu})}), \\ q^*(\sigma^2) &\sim \text{Inverse-Gamma}\left(A + \frac{n}{2}, \right. \\ &\quad \left. B + \frac{1}{2} \mu_{q(1/\sigma^2)} \left[(\mathbf{y} - \mathbf{X}\boldsymbol{\mu}_{q(\boldsymbol{\beta})})^T \mathbf{C}_{12} (\mathbf{y} - \mathbf{X}\boldsymbol{\mu}_{q(\boldsymbol{\beta})}) + \text{tr}\{\boldsymbol{\Sigma}_{q(\boldsymbol{\beta})} \mathbf{X}^T \mathbf{C}_{12} \mathbf{X}\} \right] \right), \\ q^*(a_i) &\stackrel{\text{ind.}}{\sim} \text{Inverse-Gamma}\left(\frac{\mu_{q(\nu)} + 1}{2}, \right. \\ &\quad \left. \frac{1}{2} \left[\mu_{q(\nu)} + \mu_{q(1/\sigma^2)} \{ (\mathbf{y} - \mathbf{X}\boldsymbol{\mu}_{q(\boldsymbol{\beta})})_i^2 + (\mathbf{X}\boldsymbol{\Sigma}_{q(\boldsymbol{\beta})} \mathbf{X}^T)_{ii} \} \right] \right) \\ \text{and } q^*(\nu) &= \frac{\exp \left[n \left\{ \frac{\nu}{2} \log(\nu/2) - \log \Gamma(\nu/2) \right\} - (\nu/2) C_1 \right]}{\mathcal{F}(0, n, C_1, \nu_{\min}, \nu_{\max})}, \quad \nu_{\min} < \nu < \nu_{\max}. \end{aligned} \quad (23)$$

The last density uses the same definition for C_1 that was used in the univariate case: $C_1 \equiv \sum_{i=1}^n \{ \mu_{q(\log a_i)} + \mu_{q(1/a_i)} \}$. The parameters in (23) are determined from Algorithm 7.

The lower bound on the marginal log-likelihood admits the expression:

$$\begin{aligned} \log p(\mathbf{y}; q) &= \frac{1}{2} - \frac{n}{2} \log(2\pi) + \frac{1}{2} \log |\boldsymbol{\Sigma}_\beta^{-1} \boldsymbol{\Sigma}_{q(\boldsymbol{\beta})}| \\ &\quad - \frac{1}{2} \left\{ (\boldsymbol{\mu}_{q(\boldsymbol{\beta})} - \boldsymbol{\mu}_\beta)^T \boldsymbol{\Sigma}_\beta^{-1} (\boldsymbol{\mu}_{q(\boldsymbol{\beta})} - \boldsymbol{\mu}_\beta) + \text{tr}(\boldsymbol{\Sigma}_\beta^{-1} \boldsymbol{\Sigma}_{q(\boldsymbol{\beta})}) \right\} \\ &\quad + A \log(B) - \log \Gamma(A) - (A + \frac{n}{2}) \log(B_{q(\sigma^2)}) + \log \Gamma(A + \frac{n}{2}) \\ &\quad + \log \mathcal{F}(0, n, C_1, \nu_{\min}, \nu_{\max}) - \log(\nu_{\max} - \nu_{\min}) + n \log \Gamma(\frac{1}{2}(\mu_{q(\nu)} + 1)) \\ &\quad + \frac{1}{2} \mu_{q(\nu)} \sum_{i=1}^n \mu_{q(\log a_i)} + \sum_{i=1}^n B_{q(a_i)} \mu_{q(1/a_i)} \\ &\quad - \frac{1}{2} (\mu_{q(\nu)} + 1) \sum_{i=1}^n \log \{ B_{q(a_i)} \}. \end{aligned}$$

Algorithm 7: Coordinate ascent scheme for obtaining the parameters in the optimal densities $q^*(\mathbf{a})$, $q^*(\boldsymbol{\beta})$, $q^*(\nu)$, $q^*(\sigma)$ for the t regression model.

Initialize: $\boldsymbol{\mu}_{q(\boldsymbol{\beta})} \in \mathbb{R}^{k+1}$, $\mu_{q(\nu)} \in [\nu_{\min}, \nu_{\max}]$ and $\mu_{q(1/\sigma^2)} > 0$.

Cycle:

For $i = 1, \dots, n$:

$$B_{q(a_i)} \leftarrow \frac{1}{2} [\mu_{q(\nu)} + \mu_{q(1/\sigma^2)} \{(\mathbf{y} - \mathbf{X}\boldsymbol{\mu}_{q(\boldsymbol{\beta})})_i^2 + (\mathbf{X}\boldsymbol{\Sigma}_{q(\boldsymbol{\beta})}\mathbf{X}^T)_{ii}\}]$$

$$\mu_{q(1/a_i)} \leftarrow \frac{1}{2} (\mu_{q(\nu)} + 1) / B_{q(a_i)}$$

$$\mu_{q(\log a_i)} \leftarrow \log(B_{q(a_i)}) - \text{digamma}(\frac{1}{2}(\mu_{q(\nu)} + 1))$$

$$\mathbf{C}_{12} \leftarrow \text{diag}_{1 \leq i \leq n} \{\mu_{q(1/a_i)}\} \quad ; \quad \boldsymbol{\Sigma}_{q(\boldsymbol{\beta})} \leftarrow \left\{ \mu_{q(1/\sigma^2)} \mathbf{X}^T \mathbf{C}_{12} \mathbf{X} + \boldsymbol{\Sigma}_{\boldsymbol{\beta}}^{-1} \right\}^{-1}$$

$$\boldsymbol{\mu}_{q(\boldsymbol{\beta})} \leftarrow \boldsymbol{\Sigma}_{q(\boldsymbol{\beta})} \left\{ \mu_{q(1/\sigma^2)} \mathbf{X}^T \mathbf{C}_{12} \mathbf{y} + \boldsymbol{\Sigma}_{\boldsymbol{\beta}}^{-1} \boldsymbol{\mu}_{\boldsymbol{\beta}} \right\}$$

$$C_1 \leftarrow \sum_{i=1}^n \{\mu_{q(\log a_i)} + \mu_{q(1/a_i)}\}$$

$$\mu_{q(\nu)} \leftarrow \exp\{\log \mathcal{F}(1, n, C_1, \nu_{\min}, \nu_{\max}) - \log \mathcal{F}(0, n, C_1, \nu_{\min}, \nu_{\max})\}$$

$$B_{q(\sigma^2)} \leftarrow B + \frac{1}{2} \mu_{q(1/\sigma^2)} \left[(\mathbf{y} - \mathbf{X}\boldsymbol{\mu}_{q(\boldsymbol{\beta})})^T \mathbf{C}_{12} (\mathbf{y} - \mathbf{X}\boldsymbol{\mu}_{q(\boldsymbol{\beta})}) + \text{tr}\{\boldsymbol{\Sigma}_{q(\boldsymbol{\beta})} \mathbf{X}^T \mathbf{C}_{12} \mathbf{X}\} \right]$$

$$\mu_{q(1/\sigma^2)} \leftarrow (A + \frac{n}{2}) / B_{q(\sigma^2)}$$

until the increase in $p(\mathbf{x}; q)$ is negligible.

7 Other Elaborate Response Models

Many other elaborate continuous response distributions could be entertained. Examples include Skew t (e.g., [Azzalini and Capitanio 2003](#)), Generalized Inverse Gaussian and Generalized Hyperbolic distributions. There are also numerous elaborate distributions appropriate for discrete responses, such as Negative Binomial and Beta Binomial distributions. In the multiparameter case, corresponding to Bayesian generalized additive models, the link function also impacts tractability of MFVB schemes (e.g., [Girolami and Rogers 2006](#)).

Clearly we cannot cover all possible elaborate response distributions. However, we note that the strategies used in Sections 4 to 6 involving judicious use of auxiliary variables, quadrature and finite mixture approximations apply generally. For example, equation (25) of [Azzalini and Capitanio \(2003\)](#) suggests a useful auxiliary variable representation for Skew t response models. As mentioned in Section 4.6, finite mixture approximation to the response density is always available as a last resort.

8 Accuracy Assessment

We conducted a simulation study to assess the accuracy of the univariate location-scale MFVB algorithms described in Sections 4 and 5. One hundred random samples of size $n = 500$ were drawn from the t distribution, Asymmetric Laplace, Skew Normal and Generalized Extreme Value distributions. Without loss of generality we set the location and scale parameters to be $\mu = 0$ and $\sigma = 1$. The shape parameters were:

$$\nu = 1.5 \quad \text{for the } t\text{-distribution models,}$$

$$\tau = 0.75 \quad \text{for the Asymmetric Laplace distribution model,}$$

$$\lambda = 5 \quad \text{for the Skew-Normal distribution model}$$

$$\text{and } \xi = 0.5 \quad \text{for the Generalized Extreme Value distribution model.}$$

The hyperparameters for μ were fixed at $\mu_\mu = 0$ and $\sigma_\mu^2 = 10^8$. For Inverse Gamma priors on the squared scale we used $A = B = 0.01$. For the Half Cauchy prior on the scale we used $A = 25$ and for the Log Normal prior on the scale we used $A = 100$ and $B = 10$. Shape parameter hyperparameters were $\nu_{\min} = 0.01$, $\nu_{\max} = 100$, $\mu_\lambda = 0$ and $\sigma_\lambda^2 = 10^8$. Finally, $p(\xi)$ was a uniform discrete distribution on $\Xi = \{0, 0.01, \dots, 0.99, 1\}$.

The accuracy of MFVB approximate posterior density functions was measured via

L_1 distance. Let θ be a generic parameter in any one of the models considered in Section 4 or 5. Then the L_1 error, or *integrated absolute error (IAE)* of q^* , given by

$$\text{IAE}(q^*) = \int_{-\infty}^{\infty} |q^*(\theta) - p(\theta|\mathbf{x})| d\theta.$$

Note that L_1 error is a scale-independent number between 0 and 2 and is invariant to monotone transformations on the parameter θ (Devroye and Györfi 1985). The latter property implies, for example, that the IAEs for $q^*(\sigma)$ and $q^*(\sigma^2)$ are identical. The *accuracy* of q^* is defined to be

$$\text{accuracy}(q^*) = 1 - \{\text{IAE}(q^*) / \sup_{q \text{ a density}} \text{IAE}(q)\} = 1 - \frac{1}{2} \text{IAE}(q^*). \quad (24)$$

Since $0 \leq \text{accuracy}(q^*) \leq 1$ we express this measure as a percentage in our accuracy assessments. Exact computation of $p(\theta|\mathbf{x})$ is difficult so we worked with MCMC samples obtained using BRugs (Ligges et al. 2011) with a burnin of size 10000. A thinning factor of 5 was applied to post-burnin samples of size 50000. This resulted in MCMC samples of size 10000 for density estimation. Density estimates were obtained using the binned kernel density estimate `bkde()` function in the R package `KernSmooth` (Wand and Ripley 2010). The bandwidth was chosen using a direct plug-in rule, corresponding to the default version of the `dpik()` function in `KernSmooth`.

Figure 4 summarizes the accuracy measures obtained from 100 replications of each of six models. The left-hand panels show the accuracy of MFVB for the three t models. The results are similar, regardless of form of the scale parameter prior. There is also very little between sample variability in the accuracy measures and, hence, we will simply quote average accuracy here. The location parameter μ has its posterior approximated with about 84% accuracy. For the degrees of freedom parameter ν the accuracy drops to about 71%, while it is only about 65% for the scale parameter σ . The results for the Asymmetric Laplace show an approximate reversal with the scale parameter having 74% accuracy, but the location parameter posterior at 66% accuracy. The accuracy values for the Skew Normal model are between 37% and 42% for the three model parameters μ , σ and λ , indicating that this distribution is particularly challenging for MFVB. For the Generalized Extreme Value model the location and scale have accuracy each around 50%. But the accuracy for the shape parameter ξ is excellent at 93%.

The nature of the inaccuracies is shown in Figure 5, in which the approximate densities are shown for the first replication of the simulation study. Since there is very little variability in the accuracies, these plots show typical performance. There is a pronounced tendency for the MFVB densities to be too narrow.

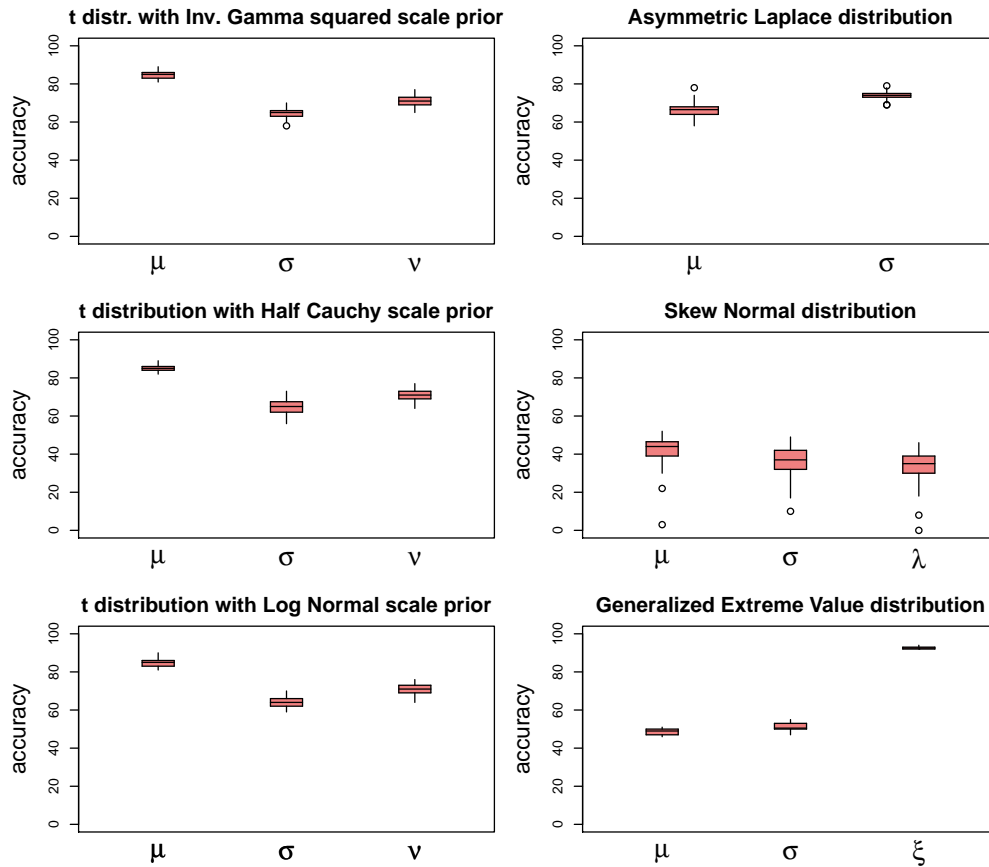


Figure 4: Boxplots of accuracy measurements for the simulation study described in the text.

Figure 6 provides some insight into why MFVB is prone to inaccuracy for the models in Sections 4–6. It shows pairwise scatterplots of the MCMC output when fitting the asymmetric Laplace model to a simulated random sample of size 100. The shape parameter was set at $\tau = 0.95$. It is apparent from Figure 6 that the posterior correlation between σ and a_1 is quite strong. The MFVB approximation with product restriction (16) ignores this dependence and, consequently, its accuracy suffers.

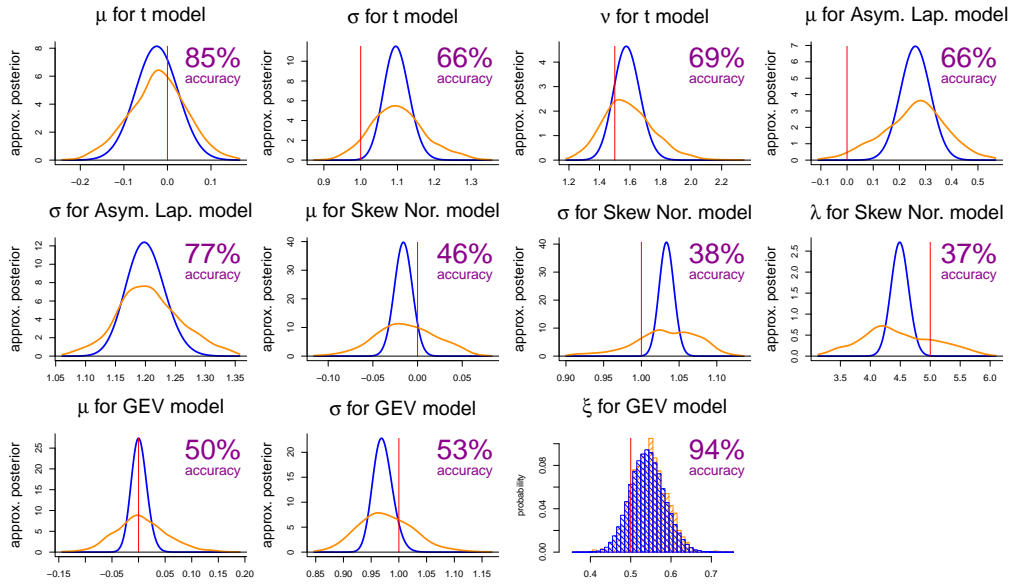


Figure 5: Comparison of MFVB and ‘exact’ (MCMC-based) posterior density functions and probability mass function for several parameters from the simulation study. In each case, the approximate posterior densities are obtained from the first replication of the simulation study. For the density function comparisons, MFVB approximations are shown as blue curves and the ‘exact’ densities are shown as orange curves. Analogous colour-coding applies to the probability mass functions.

9 Application

MFVB for elaborate distributions has enormous potential for use in applications. The locality property means that the results for the simpler models in Sections 4–6 can be used in larger models tailored to the data at hand. In this section we provide a brief illustration: robust nonparametric regression based on the t -distribution for data from a respiratory health study. The data, shown in Figure 7, correspond to measurements on one human subject during two separate respiratory experiments, during which the subject was exposed to residual oil fly ash, as part of a study conducted by Professor Russ Hauser at Harvard School of Public Health, Boston, USA. In each panel, the

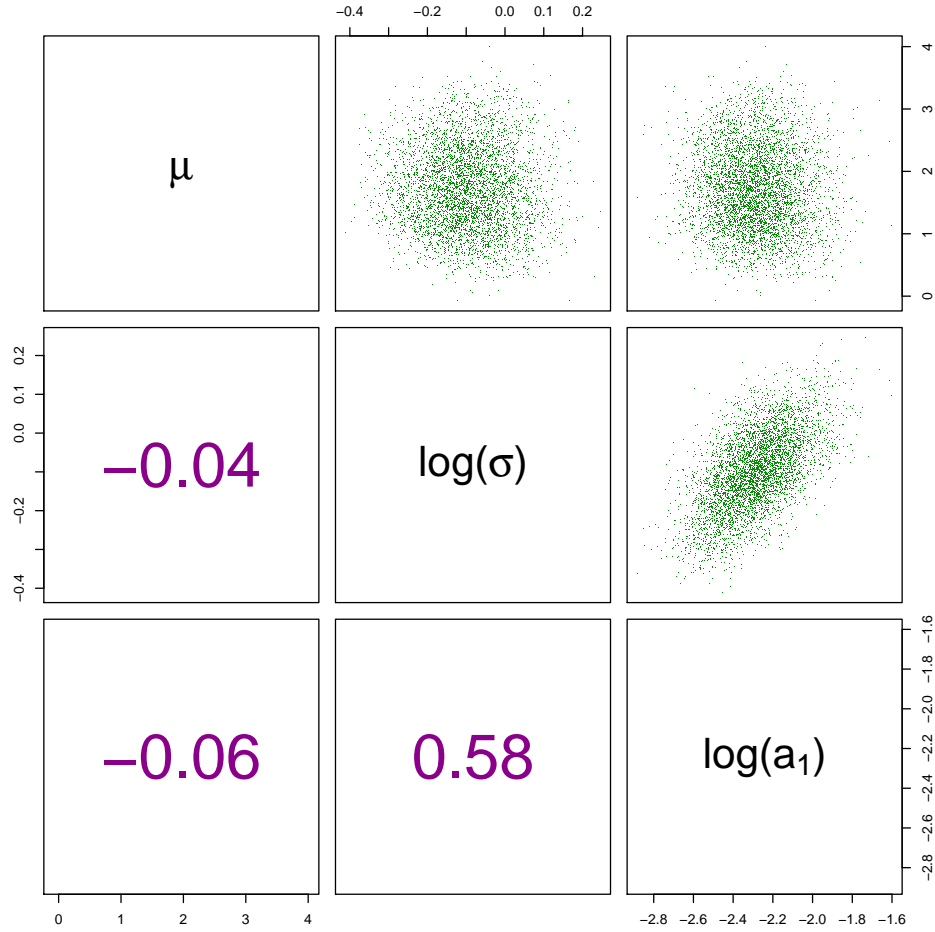


Figure 6: Pairwise scatterplots and sample correlations of MCMC output for μ , $\log(\sigma)$ and $\log(a_1)$ when fitting a univariate asymmetric Laplace model to a sample of size $n = 100$ with shape parameter $\tau = 0.95$. The MCMC sample size is 5000.

(x_i, y_i) predictor/response pairs are:

x_i = time in seconds since exposure to air containing particulate matter

y_i = $\log(\text{adjusted time of exhalation})$.

The adjusted time of exhalation is obtained by subtracting the average time of exhalation at baseline, prior to exposure to filtered air. Interest centres upon the mean response as a function of the time, so an appropriate model is

$$y_i = f(x_i) + \varepsilon_i.$$

However, the y_i s contain outlying values due to an occasional cough or sporadic breath and it is appropriate to model the errors as $\varepsilon_i \stackrel{\text{ind.}}{\sim} t(0, \sigma_\varepsilon, \nu)$. A penalized spline model for f is

$$f(x) = \beta_0 + \beta_1 x + \sum_{k=1}^K u_k z_k(x), \quad u_k \stackrel{\text{ind.}}{\sim} N(0, \sigma_u^2)$$

where $\{z_1(x), \dots, z_K(x)\}$ is an appropriate set of spline basis functions (e.g., Wand and Ormerod 2008). Staudenmayer et al. (2009) considered a non-Bayesian version of this model and described fitting via an Expectation-Maximization (EM) algorithm. Here we consider the Bayesian hierarchical model

$$y_i | \boldsymbol{\beta}, \mathbf{u}, \sigma_\varepsilon \stackrel{\text{ind.}}{\sim} t((\mathbf{X}\boldsymbol{\beta} + \mathbf{Z}\mathbf{u})_i, \sigma_\varepsilon, \nu), \quad \mathbf{u} | \sigma_u \stackrel{\text{ind.}}{\sim} N(\mathbf{0}, \sigma_u^2 \mathbf{I}),$$

$$\boldsymbol{\beta} \sim N(\mathbf{0}, \sigma_\beta^2 \mathbf{I}), \quad \sigma_\varepsilon \sim \text{Half-Cauchy}(A_\varepsilon), \tag{25}$$

$$\sigma_u \sim \text{Half-Cauchy}(A_u), \quad \nu \sim \text{Uniform}(\nu_{\min}, \nu_{\max})$$

where

$$\mathbf{X} = [1 \ x_i]_{1 \leq i \leq n} \quad \text{and} \quad \mathbf{Z} = [z_1(x_i) \ \dots \ z_K(x_i)]_{1 \leq i \leq n}.$$

We used the following product density assumption in our MFVB approximation:

$$q(\boldsymbol{\beta}, \mathbf{u}, \nu, \sigma_u, \sigma_\varepsilon) = q(\boldsymbol{\beta}, \mathbf{u}, \nu) q(\sigma_u, \sigma_\varepsilon).$$

Up until now, MFVB fitting of (25) has been challenging due to the elaborate form of the response and the non-conjugate prior distributions on the standard deviation parameters. However, simple extension of the methodology in Sections 5.1 and 6 permits its fitting. In particular, all calculations are either analytic or involve members of the $\mathcal{F}(p, q, r, s, t)$ integral family.

The hyperparameters are set at $\sigma_\beta^2 = 10^8$, $A_u = A_\varepsilon = 25$, $\nu_{\min} = 0.1$ and $\nu_{\max} = 10$ with standardized versions of the (x_i, y_i) data used in the fitting. This imposes non-informativeness for all parameters (Gelman 2006). The results were then transformed back to the original units.

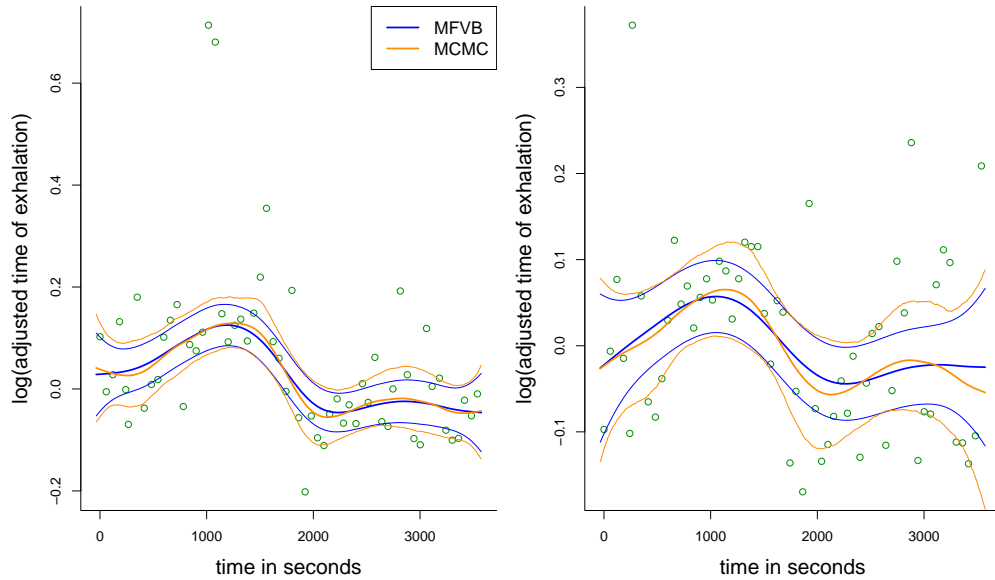


Figure 7: Comparison of MFVB and MCMC fits for robust t -based nonparametric regression, corresponding to (25). The panels correspond to measurements on one subject during two separate respiratory experiments, described in the text.

Inspection of Figure 7 shows that the MFVB fits and pointwise 95% credible sets are quite close to those obtained using MCMC (with burnin of size 15000, retained sample of size 15000, and thinning factor of 5). This high accuracy is aligned with that exhibited by $q^*(\mu)$ for the univariate t -distribution model (upper left-hand panel of Figure 4). Staudenmayer et al. (2009) admit that EM-based fitting of these data requires several hours of computing time. The MCMC fits shown in Figure 7 took 80 seconds on the first author's laptop computer (Mac OS X; 2.33 GHz processor, 3 GBytes of random access memory). A simplistic R implementation of the MFVB approximation took about 3 seconds. Lastly, we point out that the robustness gains from using t -based nonparametric regression for these data are apparent from Figure 1 of Staudenmayer et al. (2009).

10 Closing Discussion

Mean field variational Bayes provides an alternative to MCMC when speed is at a premium. In this article we have enriched significantly the class of models which can be

handled via the MFVB paradigm. The numerical studies in Section 8 show that, as with simpler distributions, MFVB for elaborate distributions entails a loss in accuracy for the convenient product restrictions used in our illustrations. Yet to be explored are less stringent product restrictions for elaborate distribution models of the type considered in Sections 4-6. These promise higher accuracy, but at the expense of higher computational overhead.

Appendix A: Derivations

The derivations in this appendix make use of the following convenient shorthand. By ‘rest’ we mean all other random variables in the Bayesian model at hand. Additive constants with respect to the function argument are denoted by ‘const’. The sample mean of x_1, \dots, x_n is denoted by $\bar{x} \equiv \frac{1}{n} \sum_{i=1}^n x_i$.

A.1. t Model

Each of the full conditional density functions satisfy:

$$\begin{aligned} \log p(\mu|\text{rest}) &= -\frac{1}{2} \left[\left\{ \frac{\sum_{i=1}^n (1/a_i)}{\sigma^2} + \frac{1}{\sigma_\mu^2} \right\} \mu^2 - 2 \left\{ \frac{\sum_{i=1}^n x_i/a_i}{\sigma^2} + \frac{\mu_\mu}{\sigma_\mu^2} \right\} \mu \right] \\ &\quad + \text{const}, \\ \log p(\sigma^2|\text{rest}) &= -(A + \frac{1}{2}n)\log(\sigma^2) - \left\{ B + \frac{1}{2} \sum_{i=1}^n \frac{(x_i - \mu)^2}{a_i} \right\} / \sigma^2 + \text{const}, \end{aligned}$$

$$\begin{aligned} \log p(\nu|\text{rest}) &= n \left\{ \frac{\nu}{2} \log(\nu/2) - \log \Gamma(\nu/2) \right\} \\ &\quad - (\nu/2) \sum_{i=1}^n \{ \log(a_i) + (1/a_i) \} + \text{const}, \quad \nu_{\min} < \nu < \nu_{\max}, \end{aligned}$$

$$\text{and } \log p(\mathbf{a}|\text{rest}) = \sum_{i=1}^n \left[-\frac{1}{2}(\nu + 1)\log(a_i) - \frac{1}{2}(1/a_i) \left\{ \nu + \frac{(x_i - \mu)^2}{\sigma^2} \right\} \right] + \text{const}.$$

Then

$$\begin{aligned} q^*(\mu) &\propto \exp\{E_{q(\sigma^2, \mathbf{a})} \log p(\mu | \text{rest})\} \\ &= \exp\left(-\frac{1}{2} \left[\left\{ \mu_{q(1/\sigma^2)} \sum_{i=1}^n \mu_{q(1/a_i)} + \frac{1}{\sigma_\mu^2} \right\} \mu^2 \right. \right. \\ &\quad \left. \left. - 2 \left\{ \mu_{q(1/\sigma^2)} \sum_{i=1}^n x_i \mu_{q(1/a_i)} + \frac{\mu_\mu}{\sigma_\mu^2} \right\} \mu \right] \right). \end{aligned}$$

Standard manipulations lead to $q^*(\mu)$ being the $N(\mu_{q(\mu)}, \sigma_{q(\mu)}^2)$ density function, where

$$\sigma_{q(\mu)}^2 = \left(\mu_{q(1/\sigma^2)} \sum_{i=1}^n \mu_{q(1/a_i)} + \frac{1}{\sigma_\mu^2} \right)^{-1}$$

and

$$\mu_{q(\mu)} = \sigma_{q(\mu)}^2 \left(\mu_{q(1/\sigma^2)} \sum_{i=1}^n x_i \mu_{q(1/a_i)} + \frac{\mu_\mu}{\sigma_\mu^2} \right).$$

The derivations for $q^*(\sigma^2)$, $q^*(\nu)$ and $q^*(\mathbf{a})$ involve similar and standard manipulations.

A.2. Asymmetric Laplace Model

The full conditionals satisfy:

$$\begin{aligned} \log p(\mu | \text{rest}) &= -\frac{1}{2} \left\{ \frac{1}{\sigma_\mu^2} + \frac{\tau(1-\tau) \sum_{i=1}^n a_i}{\sigma^2} \right\} \mu^2 \\ &\quad + \left\{ \frac{\mu_\mu}{\sigma_\mu^2} + \frac{\tau(1-\tau) \sum_{i=1}^n a_i x_i}{\sigma^2} + \frac{n(\tau - \frac{1}{2})}{\sigma} \right\} \mu + \text{const}, \\ \log p(\sigma | \text{rest}) &= -(2A + n + 1) \log(\sigma) - \frac{1}{\sigma^2} \left(B + \frac{1}{2} \tau(1-\tau) \sum_{i=1}^n a_i (x_i - \mu)^2 \right) \\ &\quad + \frac{1}{\sigma} n(\bar{x} - \mu) \left(\frac{1}{2} - \tau \right) + \text{const} \\ \text{and } \log p(\mathbf{a} | \text{rest}) &= \sum_{i=1}^n \left[-\frac{3}{2} \log(a_i) - \frac{1}{2} \left\{ a_i \frac{(x_i - \mu)^2 \tau(1-\tau)}{\sigma^2} + \frac{1}{a_i 4\tau(1-\tau)} \right\} \right] \\ &\quad + \text{const}. \end{aligned}$$

The derivation of $q^*(\mu)$ is similar to that given in Section A.1 for the t model. The optimal q -density for σ satisfies

$$q^*(\sigma) \propto \exp[E_{q(\mu, \mathbf{a})} \{p(\sigma | \text{rest})\}] = \exp(C_2/\sigma - C_3/\sigma^2), \quad \sigma > 0,$$

where

$$C_2 \equiv n(\bar{x} - \mu_{q(\mu)})(\frac{1}{2} - \tau) \quad \text{and} \quad C_3 \equiv B + \frac{1}{2}\tau(1 - \tau) \sum_{i=1}^n \mu_{q(a_i)} \{(x_i - \mu_{q(\mu)})^2 + \sigma_{q(\mu)}^2\}.$$

Noting that

$$\int_0^\infty \sigma^{-(2A+n+1+k)} \exp(C_2/\sigma - C_3/\sigma^2) d\sigma = \mathcal{J}^+(2A + n - k - 1, C_2, C_3)$$

for each of $k \in \{-2, -1, 0\}$ we get the normalizing factor for $q^*(\sigma)$ being $\mathcal{J}^+(2A + n - 1, C_2, C_3)$ and the expressions for $\mu_{q(1/\sigma^2)}$ and $\mu_{q(1/\sigma)}$ appearing in Algorithm 3. Lastly,

$$q^*(\mathbf{a}) \propto \prod_{i=1}^n a_i^{-3/2} \exp \left[-\frac{1}{2} \left\{ a_i \mu_{q(1/\sigma^2)} (x_i - \mu)^2 \tau(1 - \tau) + \frac{1}{a_i 4\tau(1 - \tau)} \right\} \right], \quad a_i > 0.$$

After a little algebra, it becomes clear that $q^*(\mathbf{a})$ is a product of Inverse Gaussian densities $q^*(a_i)$ with means

$$\mu_{q(a_i)} = \left[4\tau^2(1 - \tau)^2 \mu_{q(1/\sigma^2)} \{(x_i - \mu_{q(\mu)})^2 + \sigma_{q(\mu)}^2\} \right]^{-1/2}, \quad 1 \leq i \leq n,$$

and common precision parameter $\gamma_{q(a_i)} = \{4\tau(1 - \tau)\}^{-1}$. The expression for $\mu_{q(1/a_i)}$ in Algorithm 3 follows from the expectation results (1).

A.3. Skew Normal Model

The full conditionals satisfy

$$\begin{aligned} \log p(\mu | \text{rest}) &= -\frac{1}{2} \left\{ \frac{1}{\sigma_\mu^2} + \frac{n(1 + \lambda^2)}{\sigma^2} \right\} \mu^2 \\ &\quad + \left\{ \frac{\mu_\mu}{\sigma_\mu^2} + \frac{n(1 + \lambda^2)\bar{x}}{\sigma^2} - \frac{\lambda\sqrt{1 + \lambda^2} \sum_{i=1}^n |a_i|}{\sigma} \right\} \mu + \text{const}, \\ \log p(\sigma | \text{rest}) &= -(2A + n + 1)\log(\sigma) - \frac{1}{\sigma^2} \left(B + \frac{1}{2}(1 + \lambda^2) \sum_{i=1}^n (x_i - \mu)^2 \right) \\ &\quad + \frac{1}{\sigma} \lambda\sqrt{1 + \lambda^2} \sum_{i=1}^n |a_i|(x_i - \mu) + \text{const}, \\ \log p(\lambda | \text{rest}) &= \frac{n}{2}\log(1 + \lambda^2) - \frac{1}{2} \left[\frac{1}{\sigma^2} \sum_{i=1}^n (x_i - \mu)^2 + \sum_{i=1}^n a_i^2 + \frac{1}{\sigma_\lambda^2} \right] \lambda^2 \\ &\quad + \frac{\lambda\sqrt{1 + \lambda^2}}{\sigma} \sum_{i=1}^n |a_i|(x_i - \mu) + \frac{\mu\lambda}{\sigma_\lambda^2} + \text{const} \\ \text{and } \log p(\mathbf{a} | \text{rest}) &= \sum_{i=1}^n \left\{ -\frac{(1 + \lambda^2)a_i^2}{2} + \frac{\lambda\sqrt{1 + \lambda^2}(x_i - \mu)|a_i|}{\sigma} \right\} + \text{const}. \end{aligned}$$

The derivation for $q^*(\mu)$ is similar to that given for each of the previous models. The derivation for $q^*(\sigma)$ is similar to that given for the Asymmetric Laplace model.

To obtain $q^*(\lambda)$ note that

$$\begin{aligned} E_q\{\log p(\lambda|\text{rest})\} &= \frac{n}{2}\log(1 + \lambda^2) \\ &\quad - \frac{1}{2} \left[\mu_{q(1/\sigma^2)} \left\{ \sum_{i=1}^n (x_i - \mu_{q(\mu)})^2 + n\sigma_{q(\mu)}^2 \right\} + \sum_{i=1}^n \mu_{q(a_i^2)} + \frac{1}{\sigma_\lambda^2} \right] \lambda^2 \\ &\quad + \left[\mu_{q(1/\sigma)} \sum_{i=1}^n \mu_{q(|a_i|)} (x_i - \mu_{q(\mu)}) \right] \lambda \sqrt{1 + \lambda^2} + \frac{\mu_\lambda \lambda}{\sigma_\lambda^2} + \text{const.} \end{aligned}$$

Hence

$$q^*(\lambda) \propto (1 + \lambda^2)^{n/2} \exp \left\{ -C_6 \lambda^2 + C_7 \lambda \sqrt{1 + \lambda^2} + (\mu_\lambda / \sigma_\lambda^2) \lambda \right\}, \quad -\infty < \lambda < \infty,$$

where

$$C_6 \equiv \mu_{q(1/\sigma^2)} \left\{ \sum_{i=1}^n (x_i - \mu_{q(\mu)})^2 + n\sigma_{q(\mu)}^2 \right\} + \sum_{i=1}^n \mu_{q(a_i^2)} + \frac{1}{\sigma_\lambda^2}$$

and

$$C_7 \equiv \mu_{q(1/\sigma)} \sum_{i=1}^n \mu_{q(|a_i|)} (x_i - \mu_{q(\mu)}).$$

The normalizing factor is

$$\begin{aligned} &\int_{-\infty}^{\infty} (1 + \lambda^2)^{n/2} \exp \left\{ -C_6 \lambda^2 + C_7 \lambda \sqrt{1 + \lambda^2} + (\mu_\lambda / \sigma_\lambda^2) \lambda \right\} d\lambda \\ &= \mathcal{G}(0, \frac{1}{2}n, \frac{1}{2}C_6, C_7, (\mu_\lambda / \sigma_\lambda^2)). \end{aligned}$$

The expressions for $\mu_{q(\lambda^2)}$ and $\mu_{q(\lambda\sqrt{1+\lambda^2})}$ involve similar manipulations. Finally,

$$\begin{aligned} E_{q(\mu, \sigma, \lambda)}\{\log p(\mathbf{a}|\text{rest})\} &= \\ &\sum_{i=1}^n \left\{ -\frac{1}{2}(1 + \mu_{q(\lambda^2)})a_i^2 + \mu_{q(1/\sigma)} \mu_{q(\lambda\sqrt{1+\lambda^2})} (x_i - \mu_{q(\mu)}) |a_i| \right\} + \text{const.} \end{aligned}$$

Hence,

$$q^*(\mathbf{a}) \propto \prod_{i=1}^n \exp \left\{ -\frac{1}{2}(1 + \mu_{q(\lambda^2)})a_i^2 + C_{i8} |a_i| \right\}, \quad -\infty < a_i < \infty, \quad 1 \leq i \leq n,$$

where

$$C_{i8} \equiv \mu_{q(1/\sigma)} \mu_{q(\lambda\sqrt{1+\lambda^2})} (x_i - \mu_{q(\mu)}).$$

The normalizing factors and moment expressions follow from standard manipulations involving the normal density and cumulative distribution functions.

A.4. Finite Normal Mixture Model

The full conditionals satisfy:

$$\begin{aligned} \log p(\mu|\text{rest}) &= -\frac{1}{2} \left[\left\{ \frac{1}{\sigma^2} \sum_{k=1}^K \frac{a_{\bullet k}}{s_k^2} + \frac{1}{\sigma_\mu^2} \right\} \mu^2 \right. \\ &\quad \left. - 2 \left\{ \frac{1}{\sigma^2} \sum_{i=1}^n \sum_{k=1}^K \frac{a_{ik} x_i}{s_k^2} - \frac{1}{\sigma} \sum_{k=1}^K \frac{a_{\bullet k} m_k}{s_k^2} + \frac{\mu_\mu}{\sigma_\mu^2} \right\} \mu \right] \\ &\quad + \text{const} \\ \log p(\sigma|\text{rest}) &= -(2A + n + 1) \log(\sigma) - \frac{1}{\sigma^2} \left\{ B + \frac{1}{2} \sum_{i=1}^n \sum_{k=1}^K \frac{a_{ik} (x_i - \mu)^2}{s_k^2} \right\} \\ &\quad + \frac{1}{\sigma} \sum_{i=1}^n \sum_{k=1}^K \frac{a_{ik} m_k (x_i - \mu)}{s_k^2} + \text{const} \\ \text{and } \log p(\mathbf{a}|\text{rest}) &= \sum_{i=1}^n \sum_{k=1}^K a_{ik} \left\{ \log(w_k) - \frac{1}{2} \log(s_k^2) - \frac{(x_i - \mu - \sigma m_k)^2}{2\sigma^2 s_k^2} \right\} + \text{const} \end{aligned}$$

where $a_{\bullet k} \equiv \sum_{i=1}^n a_{ik}$. The derivation for $q^*(\mu)$ is similar to that given for each of the previous models. The derivation for $q^*(\sigma)$ is similar to that given for the Asymmetric Laplace and Skew Normal models. To obtain $q^*(\mathbf{a})$, first note that

$$E_{q(\mu, \sigma)} \{ \log p(\mathbf{a}|\text{rest}) \} = \sum_{i=1}^n \sum_{k=1}^K a_{ik} \nu_{ik} + \text{const}$$

where ν_{ik} is given in Algorithm 5. It follows that $q^*(\mathbf{a}) \propto \prod_{i=1}^n \prod_{k=1}^K \{ \exp(\nu_{ik}) \}^{a_{ik}}$. The requirement that $\sum_{k=1}^K \mu_{q(a_{ik})} = 1$ for all $1 \leq i \leq n$ then leads to

$$q^*(\mathbf{a}) = \prod_{i=1}^n \prod_{k=1}^K \{ \mu_{q(a_{ik})} \}^{a_{ik}} \quad \text{where} \quad \mu_{q(a_{ik})} = \exp(\nu_{ik}) / \sum_{k=1}^K \exp(\nu_{ik}).$$

Appendix B: Numerical Integration

Many of the non-analytic integrals that arise in variational Bayes for elaborate distributions are of the form

$$\mathcal{I}(\boldsymbol{\theta}) = \int_a^b \exp\{h(x; \boldsymbol{\theta})\} dx$$

where $h''(x; \boldsymbol{\theta}) < 0$ for all $a < x < b$ and $\boldsymbol{\theta}$. In other words, the integrand is *log-concave* over the domain for all values of its parameters which, as explained in Appendix B.1., aids numerical integration strategies. This is the case for the integral families $\mathcal{J}(p, q, r, s)$

and $\mathcal{J}^+(p, q, r)$ defined in Section 2.1. The family $\mathcal{F}(p, q, r, s, t)$ does not have this property, so needs to be treated more carefully. We will give the details for log-concave integrands.

The value of $\mathcal{I}(\boldsymbol{\theta})$ can be arbitrarily small or large for various values of $\boldsymbol{\theta}$. Hence, it is prudent to work with $\log\{\mathcal{I}(\boldsymbol{\theta})\}$ instead, to avoid underflow and overflow.

B.1. Transforming the integrand to a ‘nice’ scale

In this section, we suppress the dependence of \mathcal{I} and h on the parameters $\boldsymbol{\theta}$. We transform the integrand to a nice scale by borrowing from the ideas of Laplace approximation and Gauss-Hermite quadrature (e.g., Liu and Pierce 1994). The log-concavity property means that the equation

$$h'(x) = 0$$

has a unique solution. Using the ideas of Laplace approximation, we use the substitution

$$u = \frac{x - \mu_0}{\sigma_0 \sqrt{2}}$$

where

$$\mu_0 \equiv \text{the solution to } h'(x) = 0 \quad \text{and} \quad \sigma_0 \equiv 1/\sqrt{-h''(\mu_0)}.$$

These choices aim to make the integrand close to a multiple of the standard normal density function. On substitution into the $\log\mathcal{I}$ expression we get

$$\log\mathcal{I} = h(\mu_0) + \log(\sigma_0 \sqrt{2}) + \log(\mathcal{I}_0)$$

where

$$\mathcal{I}_0 \equiv \int_{(a-\mu_0)/(\sigma_0 \sqrt{2})}^{(b-\mu_0)/(\sigma_0 \sqrt{2})} \exp\{h(\mu_0 + u \sigma_0 \sqrt{2}) - h(\mu_0)\} du.$$

B.2. Quadrature for \mathcal{I}_0

We have now reduced the problem to one involving numerical integration for \mathcal{I}_0 . The integrand for \mathcal{I}_0 has the properties of being unimodal, bounded above by unity and has support ‘similar’ to the standard normal density. For the families $\mathcal{G}(p, q, r, s, t)$, $\mathcal{J}(p, q, r, s)$ and $\mathcal{J}^+(p, q, r)$ the integrands have exponentially decaying tails. Therefore, even simple quadrature such as the trapezoidal or Simpson’s rules can be very accurate provided we (a) determine the effective support of the integrand; and (b) use a high

number of quadrature points. For (a) a reasonable way to do this is to sequentially enlarge the support (L, U) until

$$\max\{\exp\{h(\mu_0 + L\sigma_0\sqrt{2}) - h(\mu_0)\}, \exp\{h(\mu_0 + U\sigma_0\sqrt{2}) - h(\mu_0)\}\} < \varepsilon$$

for some ‘small’ ε such as 10^{-15} . For (b) we use doubling of the number of quadrature points until the relative error is below some nominal threshold such as 10^{-5} .

Appendix C: Finite Normal Mixture Approximation

In this appendix we describe our strategy for finite normal mixture approximation of Generalized Extreme Value density functions, as required for Algorithm 6.

Recall that the GEV(0, 1, ξ) family of density functions is given by

$$f(x; \xi) = \begin{cases} (1 + \xi x)^{-1/\xi-1} e^{-(1+\xi x)^{-1/\xi}}, & 1 + \xi x > 0, \xi \neq 0 \\ \exp(-x - e^{-x}), & \xi = 0. \end{cases}$$

The support is $[-1/\xi, \infty)$ for $\xi > 0$, \mathbb{R} for $\xi = 0$ and $(-\infty, -1/\xi]$ for $\xi < 0$. For $\xi = -1$ the density function has a jump discontinuity at $x = 1$ and for $\xi < -1$ it has a pole at $x = -1/\xi$. In the present article we have restricted attention to $-1 \leq \xi \leq 1$. In applications, this sub-family is usually found to be adequate for modelling sample extremes.

Let

$$f^{NM}(x; \mathbf{w}_{\xi, \xi}, \mathbf{s}_{\xi}) \equiv \sum_{k=1}^K \frac{w_{k, \xi}}{s_{k, \xi}} \phi\left(\frac{x - m_{k, \xi}}{s_{k, \xi}}\right)$$

be a normal mixture approximation to $f(x; \xi)$. The notation is the same as that used in Table 1, with the addition of a ξ subscript. After fixing K , we considered choice of $(\mathbf{w}_{\xi, \xi}, \mathbf{s}_{\xi})$ by minimizing both L_1 distance:

$$\text{IAE}(\mathbf{w}_{\xi, \xi}, \mathbf{s}_{\xi}; \xi) \equiv \int_{-\infty}^{\infty} |f^{NM}(x; \mathbf{w}_{\xi, \xi}, \mathbf{s}_{\xi}) - f(x; \xi)| dx$$

and χ^2 distance

$$\chi^2(\mathbf{w}_{\xi, \xi}, \mathbf{s}_{\xi}; \xi) \equiv \int_S \{f^{NM}(x; \mathbf{w}_{\xi, \xi}, \mathbf{s}_{\xi}) - f(x; \xi)\}^2 / f^{NM}(x; \mathbf{w}_{\xi, \xi}, \mathbf{s}_{\xi}) dx$$

where S is the effective support of $f^{NM}(\cdot; \mathbf{w}_{\xi, \xi}, \mathbf{s}_{\xi})$. The Nelder-Mead simplex algorithm (Nelder and Mead 1965) was used for optimization via the MATLAB function

`fminsearch`. The entries of \mathbf{w}_ξ were constrained to be at least 10^{-6} . The component means and variances were constrained to compact intervals. The algorithm was terminated after convergence to a local minimum.

The integrals were approximated using the trapezoidal rule on an adaptive grid. For $\xi < 0$ we used 540 grid points to the left of the mode at $x = \{(1+\xi)^{-\xi} - 1\}/\xi$ and 540 grid points between the mode at the upper end of the support at $x = -1/\xi$. An additional 120 grid points were used in the interval $[-1/\xi, -1/\xi + 4]$ since $f^{\text{NM}}(\cdot; \mathbf{w}_{\xi, \xi}, \mathbf{s}_\xi)$ may have a small amount of probability mass above $-1/\xi$. For $\xi \geq 0$ the grid point strategy required more care due to the heavy right-hand tail. An equi-spaced grid between the 10^{-8} and $1 - 10^{-6}$ quantiles of $f^{\text{NM}}(\cdot; \mathbf{w}_{\xi, \xi}, \mathbf{s}_\xi)$, but right-truncated at 100000, was used. The grid sizes increased linearly from 1100 for $\xi = 0$ to 7500 for $\xi = 0.3$ and were fixed at 7500 for $0.3 < \xi \leq 1$. Approximating mixtures were determined for $\xi \in [-1, 1]$ over an equally-spaced grid of size 401.

Figure 8 shows some indications of the accuracy of $K = 24$ mixture normal mixture approximations to the $f(\cdot; \xi)$ density functions. The top panel shows the accuracy of the L_1 -based approximation. Since the L_1 distance between two density functions is a scale-independent number between 0 and 2, the vertical axis is immediately meaningful. The fact that the L_1 distance is uniformly below 0.01 implies that the accuracy measure defined by (24) always exceeds 99.5%. The second panel shows accuracy of χ^2 -based approximation. The bottom panel compares the two types of approximation in terms of Kullback-Leibler distance and shows that the χ^2 -based approximation is almost uniformly better. Further error analyses reveal that χ^2 distance leads to better accuracy in the tails. This is particularly important for $\xi > 0$ since the upper tail of $f(\cdot; \xi)$ is heavy compared with those of normal densities. Hence, we recommend the χ^2 -based normal mixture approximations and these are used in Section 4.5.

A text file containing the fitted normal parameters over the fine grid of ξ values is available as web-supplement to this article.

References

Aigner, D. J., Lovell, C. A. K., and Schmidt, P. (1977). "Formulation and estimation of stochastic frontier production function models." *Journal of Econometrics*, 12: 21–37.

856

Antoniadis, A. and Fan, J. (2001). "Regularization of wavelet approximations (with

- discussion).” *Journal of the American Statistical Association*, 96: 939–967. 865
- Archanbeau, C. and Bach, F. (2008). “Sparse probabilistic projections.” In *21st Annual Conference on Neural Information Processing Systems*, 73–80. Vancouver, Canada. 849
- Armagan, A. (2009). “Variational bridge regression.” *Journal of Machine Learning Research, Workshop and Conference Proceedings*, 5: 17–24. 849
- Attias, H. (1999). “Inferring parameters and structure of latent variable models by variational Bayes.” In *Proceedings of the 15th Conference on Uncertainty in Artificial Intelligence*, 21–30. 848
- Azzalini, A. and Capitanio, A. (2003). “Distributions generated by perturbation of symmetry with emphasis on a multivariate skew t-distribution.” *Journal of the Royal Statistical Society, Series B*, 65: 367–389. 880
- Azzalini, A. and Dalla Valle, A. (1996). “The multivariate skew-normal distribution.” *Biometrika*, 83: 715–726. 856, 867
- Bishop, C. M. (2006). *Pattern Recognition and Machine Learning*. New York: Springer. 856, 858
- Braun, M. and McAuliffe, J. (2010). “Variational inference for large-scale models of discrete choice.” *Journal of the American Statistical Association*, 105: 324–335. 850
- Chib, S., Nardari, F., and Shephard, N. (2002). “Markov chain Monte Carlo methods for stochastic volatility models.” *Journal of Econometrics*, 108: 281–316. 850
- Consonni, G. and Marin, J.-M. (2007). “Mean-field variational approximate Bayesian inference for latent variable models.” *Computational Statistics and Data Analysis*, 52: 790–798. 849
- Cottet, R., Kohn, R. J., and Nott, D. J. (2008). “Variable selection and model averaging in semiparametric overdispersed generalized linear models.” *Journal of the American Statistical Association*, 103: 661–671. 875
- Devroye, L. and Györfi, L. (1985). *Density Estimation: The L_1 View*. New York: Wiley. 881
- Frühwirth-Schnatter, S. and Frühwirth, R. (2010). “Data augmentation and MCMC for binary and multinomial logit models.” In Kneib, T. and Tutz, G. (eds.), *Statistical*

- Modelling and Regression Structures – Festschrift in Honour of Ludwig Fahrmeir*, 111–132. Heidelberg, Germany: Physica-Verlag. 850
- Frühwirth-Schnatter, S., Frühwirth, R., Held, L., and Rue, H. (2009). “Improved auxiliary mixture sampling for hierarchical models of non-Gaussian data.” *Statistics and Computing*, 19: 479–492. 850, 873
- Frühwirth-Schnatter, S. and Wagner, H. (2006). “Auxiliary mixture sampling for parameter driven models of time series counts with applications to state space modelling.” *Biometrika*, 93: 827–841. 873
- Gelman, A. (2006). “Prior distributions for variance parameters in hierarchical models.” *Bayesian Analysis*, 1: 515–533. 862, 875, 885
- Girolami, M. and Rogers, S. (2006). “Variational Bayesian multinomial probit regression.” *Neural Computation*, 18: 1790–1817. 849, 880
- Gradshteyn, I. S. and Ryzhik, I. M. (1994). *Tables of Integrals, Series, and Products*. San Diego, California: Academic Press, 5th edition. 852
- Jaakkola, T. S. (2001). “Tutorial on variational approximation methods.” In Opper, M. and Saad, D. (eds.), *Advanced Mean Field Methods: Theory and Practice*, 129–160. Cambridge, Massachusetts: MIT Press. 860
- Jordan, M. I., Ghahramani, Z., Jaakkola, T. S., and Saul, L. K. (1999). “An introduction to variational methods for graphical models.” *Machine Learning*, 37: 183–233. 848
- Kim, S., Shephard, N., and Chib, S. (1998). “Stochastic volatility: Likelihood inference and comparison with ARCH models.” *Review of Economic Studies*, 65: 361–393. 850
- Kotz, S., Kozubowski, T. J., and Podgórski, K. (2001). *The Laplace Distribution and Generalizations*. Boston: Birkhäuser. 855
- Kschischang, F. R., Frey, B. J., and Loeliger, H.-A. (2001). “Factor graphs and the sum-product algorithm.” *IEEE Transactions on Information Theory*, 47: 498–519. 848
- Lange, K. L., Little, R. J. A., and Taylor, J. M. G. (1989). “Robust statistical modeling using the t distribution.” *Journal of the American Statistical Association*, 84: 881–896. 855, 863, 878
- Lasserre, J. B. (2001). “Global optimization with polynomials and problem of moments.” *SIAM Journal of Optimization*, 12: 756–769. 848

- Ligges, U., Thomas, A., Spiegelhalter, D., Best, N., Lunn, D., Rice, K., and Sturtz, S. (2011). *BRugs 0.5: OpenBUGS and its R/S-PLUS interface BRugs*.
URL <http://www.stats.ox.ac.uk/pub/RWin/src/contrib/> 881
- Liu, Q. and Pierce, D. A. (1994). “A note on Gauss-Hermite quadrature.” *Biometrika*, 81: 624–629. 892
- Luenberger, D. G. and Ye, Y. (2008). *Linear and Nonlinear Programming*. New York: Springer, 3rd edition. 858
- Lunn, D., Thomas, A., Best, N. G., and Spiegelhalter, D. J. (2000). “WinBUGS – A Bayesian Modelling Framework: Concepts, Structure, and Extensibility.” *Statistics and Computing*, 10: 325–337. 848
- Marron, J. S. and Wand, M. P. (1992). “Exact mean integrated squared error.” *The Annals of Statistics*, 20: 712–736. 853, 854
- McGrory, C. A. and Titterton, D. M. (2007). “Variational approximations in Bayesian model selection for finite mixture distributions.” *Computational Statistics and Data Analysis*, 51: 5352–5367. 848
- Minka, T. (2001). “Expectation propagation and approximate Bayesian inference.” In *Proceedings on the 17th Conference on Uncertainty in Artificial Intelligence*, 362–369. San Francisco: Morgan Kaufmann. 848
- Minka, T., Winn, J., Guiver, G., and Knowles, D. (2010). “Infer.NET 2.4.” Microsoft Research Cambridge.
URL <http://research/microsoft.com/infernet> 848
- Nelder, J. and Mead, R. (1965). “A simplex method for function minimization.” *Computer Journal*, 7: 308–313. 893
- Omori, Y., Chib, S., Shephard, N., and Nakajima, J. (2007). “Stochastic volatility with leverage: Fast and efficient likelihood inference.” *Journal of Econometrics*, 140: 425–449. 850
- Ormerod, J. T. and Wand, M. P. (2010). “Explaining variational approximations.” *The American Statistician*, 64: 140–153. 848, 858, 860, 861
- Parisi, G. (1988). *Statistical Field Theory*. Redwood City, California: Addison-Wesley. 848

- Park, T. and Casella, G. (2008). “The Bayesian lasso.” *Journal of the American Statistical Association*, 103: 681–686. 865
- Pearl, J. (1988). *Probabilistic Reasoning in Intelligent Systems*. San Mateo, California: Morgan Kaufmann. 859
- Saul, L. K. and Jordan, M. I. (1996). “Exploiting tractable substructures in intractable networks.” In *Advances in Neural Information Processing Systems*, 435–442. Cambridge, Massachusetts: MIT Press. 860
- Shephard, N. (1994). “Partial non-Gaussian state space.” *Biometrika*, 81: 115–131. 850
- Staudenmayer, J., Lake, E. E., and Wand, M. P. (2009). “Robustness for general design mixed models using the t -distribution.” *Statistical Modelling*, 9: 235–255. 885, 886
- Teschendorff, A. E., Wang, Y., Barbosa-Morais, N. L., Brenton, J. D., and Caldas, C. (2005). “A variational Bayesian mixture modelling framework for cluster analysis of gene-expression data.” *Bioinformatics*, 21: 3025–3033. 848
- Tipping, M. E. and Lawrence, N. D. (2003). “A variational approach to robust Bayesian interpolation.” *IEEE Workshop on Neural Networks for Signal Processing*, 229–238. 849
- Wainwright, M. J. and Jordan, M. I. (2008). “Graphical models, exponential families, and variational inference.” *Foundation and Trends in Machine Learning*, 1: 1–305. 848, 858
- Wand, M. P. and Ormerod, J. T. (2008). “On semiparametric regression with O’Sullivan penalized splines.” *Australian and New Zealand Journal of Statistics*, 50: 179–198. 885
- Wand, M. P. and Ripley, B. D. (2010). *KernSmooth 2.23: Functions for kernel smoothing corresponding to the book: Wand, M.P. and Jones, M.C. (1995) “Kernel Smoothing”*.
URL <http://cran.r-project.org> 881
- Wang, B. and Titterton, D. M. (2005). “Inadequacy of interval estimates corresponding to variational Bayesian approximations.” In Cowell, R. and Ghahramani, Z. (eds.), *Proceedings of the 10th International Workshop on Artificial Intelligence and Statistics*, 373–380. 850

Winn, J. and Bishop, C. M. (2005). “Variational message passing.” *Journal of Machine Learning Research*, 6: 661–694. [849](#)

Yu, K. and Moyeed, R. A. (2001). “Bayesian quantile regression.” *Statistics and Probability Letters*, 54: 437–447. [865](#)

Zhang, S. and Jin, J.-M. (1996). *Computation of Special Functions*. New York: Wiley. [852](#)

Acknowledgments

The first author is grateful to Professor A.C. Davison and the Department of Mathematics at the Swiss Federal Institute of Technology, Lausanne, Switzerland, for their hospitality during the early stages of this research. We thank Sarah Neville and Shen Wang for their assistance with some of the derivations. We are also grateful for comments received from an editor and two referees which resulted in considerable improvement of this article. This research was partially supported by Australian Research Council Discovery Projects DP0877055 and DP110100061 and by the EXTREMES project of the Competence Center Environment and Sustainability, Swiss Federal Institute of Technology, Lausanne, Switzerland.

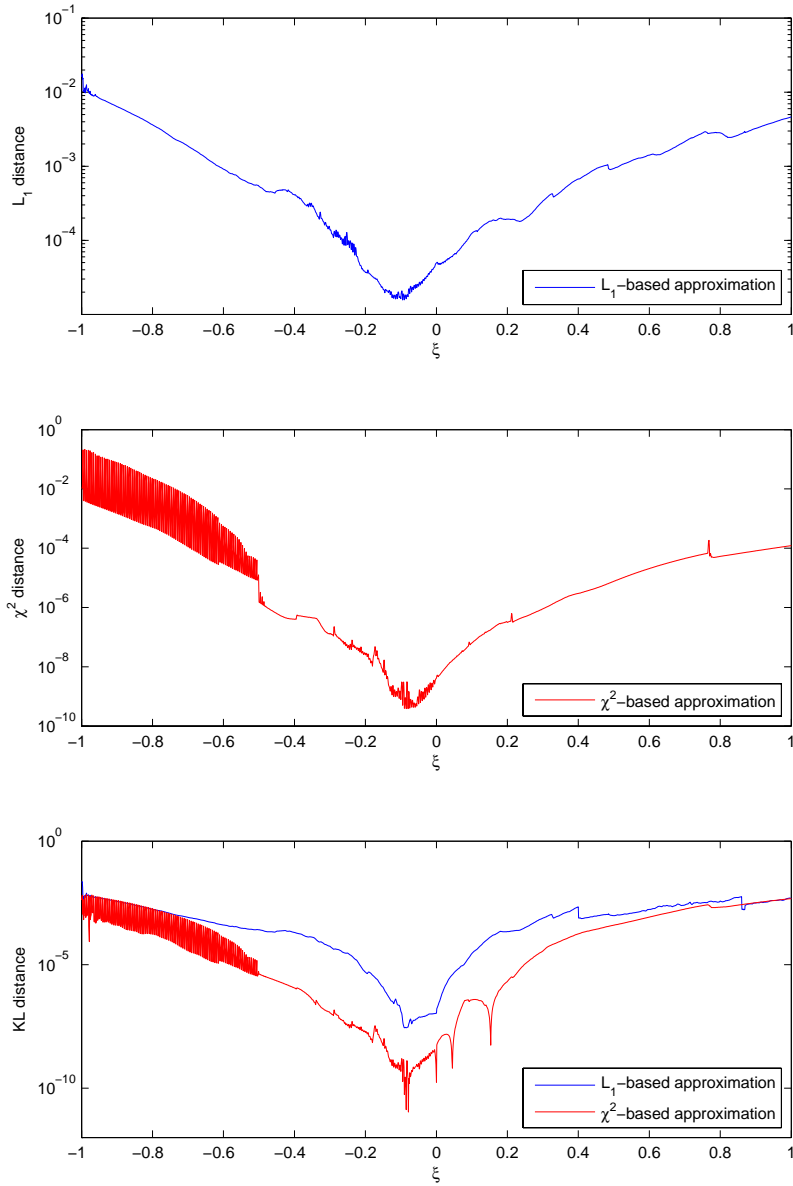


Figure 8: Accuracy of both L_1 -based and χ^2 -based approximation to $GEV(0, 1, \xi)$ density functions using $K = 24$ normal mixtures. The top panel plots L_1 distance versus $-1 \leq \xi \leq 1$ for L_1 -based approximation. The second panel shows an analogous plot for χ^2 distance. The bottom panel plots Kullback-Leibler distance versus $-1 \leq \xi \leq 1$ for both types of approximation.